Nanoscale Advances

ROYAL SOCIETY OF CHEMISTRY

REVIEW

View Article Online
View Journal | View Issue

Cite this: *Nanoscale Adv.*, 2020, **2**, 1774

Ecofriendly ruthenium-containing nanomaterials: synthesis, characterization, electrochemistry, bioactivity and catalysis†

Pranshu K. Gupta and Lallan Mishra *

Among transition metals, ruthenium being an in-demand element along with its complexes with multidimensional applications in biology, catalysis (especially photocatalysis), and several other aspects of industrial materials, is lacking regards for the potential aspect of its nanoparticles. In the modern synthetic scenario, green synthesis of novel ruthenium nanoparticles for the development of novel materials with potential applications has become a focus. Ru-containing nanomaterials (Ru-cNMs) combined with metals like platinum and palladium or with non-metals like phosphorus and oxygen have shown applications as an anticancer, antimicrobial, and antioxidant agents along with wide-ranging catalytic applications. Reduction of Ru salts using biomaterials including plants *etc.* has emerged enabling the synthesis of Ru-cNMs. In this context, authors realize that poor availability of literature in this area of research seems to be one of the major handicaps that perhaps could be limiting its attractiveness to researchers. Therefore, it was thought worthwhile to present a review article to encourage, guide, and facilitate scientific researches in green ruthenium nanochemistry embodying synthesis, characterization and biological as well as catalytic applications.

Received 20th January 2020
Accepted 27th March 2020

DOI: 10.1039/d0na00051e

rsc.li/nanoscale-advances

Department of Chemistry, Institute of Science, Banaras Hindu University, Varanasi-221005, India. E-mail: lmishrabhu@yahoo.co.in

† Electronic supplementary information (ESI) available. See DOI: 10.1039/d0na00051e

Introduction

The world is facing three major crises, namely pollution, energy and cancer. Pollution and chemical wastes have already crossed

Pranshu Kumar Gupta has been BSc (Hons.) Gold-Medalist in Chemistry, and is pursuing his MSc degree in chemistry (inorganic chemistry) from the Institute of Science, Banaras Hindu University (BHU), Varanasi, India. He has worked as a summer research fellow at the Indian Institute Science (IISc, Bangalore) and Indian Institute of Scientific Education and Research (IISER, Thiruvananthpuram) under the supervision of eminent scientists. He is presently working as a project student under the guidance of Prof. Lallan Mishra, at the Department of Chemistry (CAS), BHU, India. His research interests are in nanochemistry, development of eco-friendly metal nanoparticles and carbon quantum dots: metal/bio-stabilizer induced bioactivity surface-enhanced catalysis and quantum confinement-based photochemistry.

Prof. (Distin.) Lallan Mishra (FRSC) is presently working as a Distinguished Professor in Chemistry at the Chemistry Department, Banaras Hindu University, India. He joined this department in 1988 and was also the Head of Department during 2013–15. Prof. Mishra obtained his PhD from DDU Gorakhpur, India and had pursued post-doctoral work at IISc Bangalore, IIT Kanpur India and the University of Antwerp, Belgium in 1982, 1985 and 1986 respectively. He has supervised more than 20 doctoral students and authored more than 150 peer-reviewed journal articles. His research interests are in bioinorganic and supramolecular chemistry, metal-based anticancer drugs, chemo/bio/nano-sensors for biologically relevant cations and anions and coordination chemistry with a special focus on architectural aspects and functional materials.

their danger limits. We urgently need materials that can fulfil commercial demands by posing a minimum risk to civilization and the environment. Moreover, they should be accessible, affordable, qualitative and quantitative in activity. These issues certainly have turned out to be a big challenge for modern-day scientists irrespective of their scientific disciplines. Chemistry being at the heart of all sciences has attempted significantly to overcome these issues, through novel technologies like hydrogen fuel systems, oxygen-evolving systems, energy-conserving catalysts, and anticancer drugs. Nanotechnology has emerged as a multidimensional field of research, whose applications extend over physical, chemical and biological sciences. Nanoparticles (NPs) being materials of modern-day science have been synthesized either through bottom-up or top-down approaches, which are no doubt most exploited, but are cumbersome, hazardous and pose an elevated threat in terms of the environment, cost and energy. Pollution-free or "green" chemistry seems fascinating as its technology inclines towards materials of natural origin, hence enhancing their significance.[1]

Torresday *et al.* combined nanotechnology and green chemistry by developing a protocol for the synthesis of Ag NPs by exploiting bio-extracts of plant or other microbial origins, hence promoting the synthetic strategy to a more quantitative, qualitative, and environment-friendly level.[2] The capability to synthesize monodispersed metal NPs, in an affordable, eco-friendly and tailored format catered to the needs of the time, paving the way for numerous publications, and evolving newer aspects of green synthesis. However, these publications and reports are much more inclined towards Ag and Au NPs, because of their facile synthesis.[3] These metals no doubt possess biological relevance, but catalytically they were found to be inefficient owing to their low coordination numbers. Other metals, particularly those near to the Mn group, turned out to be catalytically relevant metals for commercially exploitable reduction catalysis. Being cheaper than Pt, Pd and Ir, Ru turned out to be an affordable metal for catalytic and optoelectronic studies.[4] Ligand field calculations support its tedious synthesis but facile capping, enabling ligand transfer reactions of Ru NPs.[5] This enthused researchers towards Ru-based organometallic complexes, and Ru NPs showing significant catalytic efficiency. However, studies done during that time posed problems like excessive chemical waste generation, energy issues, insufficient ligand transfer, toxic synthetic strategies, tedious stoichiometric control, pH sensitivity and unsatisfactory catalytic parameters like yield, selectivity and recycling ability.[6]

In 2012, Srivastava and co-workers reported bacterial-extract-mediated synthesis of metal NPs including those of Ru.[7] This encouraged green synthesis of metal NPs and their catalytic and biological studies. Green bioextract-mediated Ru NPs were tested through catalytic and bioactivity assays. They were later found to be a potent catalyst and significant antibacterial and anticancer agents.[8] Recently (2019), we have established their efficient antifungal and antioxidant activity.[9] Catalytic and supercapacitor activities of these NPs were also studied.[10] Significant changes came in the field of transition metal green nanochemistry. Monodispersed Ru-containing nanomaterials (Ru-cNMs) could now be synthesized by environment-friendly, less toxic and less energetically intensive modes of synthesis, with facile ligand transfer owing to biostabilizer generated heteroleptic ligand distortion. These nanocatalysts generated less chemical wastes and gave significant yield, selectivity, and recyclability. Bioextract-based Ru-cNMs can efficiently solve all the mentioned problems. Over recent years, publications on bioextract-mediated Ru-cNMs have revealed their immense capabilities in some of the most peculiar domains of chemical, physical, and biological sciences. Studies on chemically synthesized Ru and RuO_2 NPs have been done, involving direct methanol fuel cells, supercapacitor electrodes, chem-iluminescence, anticancer activity, synthesis and degradation catalysis.[11] RuO_2 NPs are popular due to their redox properties, conductance, *etc.* They have been employed as electrodes in charge accumulating systems, and chlor-alkali units. The physicochemical properties of Ru and RuO_2 NPs are well established, but their green synthesis, bioactivity and catalysis are still at an early stage. Until 2012, there were no communications regarding them, but in the last 7–8 years, some successful efforts have been made. As depicted in Scheme 1, these ecofriendly synthesized Ru-cNMs have been shown to be able to reduce aromatic compounds and other functional groups, catalyze water-splitting reactions, reactivate methanol fuel cells, and exhibit bioactivity such as antimicrobial, anti-oxidative and anticancer properties.

This review could be considered a "first review" in many contexts, to the best of our knowledge. This is the first review on green synthesis of Ru-cNMs that covers all relevant literature to 2019. It also covers the wider range of Ru-cNMs reported so far. An attempt has been made to critically review both biological and physicochemical aspects in a comprehensive manner to provide all relevant information about Ru NPs in one place. To the best of our knowledge, no other reviews in this area are available dealing with a wider span of Ru NPs. This review aims to classify Ru-cNMs on the basis of composition, synthetic strategy and biochemical applications. Moreover, this review deals with the novel concept of nanoparticles-plant group (NPs-Pg) correlation plot that has been recently reported by us. This method formulates a better understanding of NP size-bioactivity correlation. A more comprehensive discussion of its graphical parameters has been taken up to explain the wider scope of this plot. It not only guides but also assists young researchers in work on Ru-cNMs. Being a preliminary review on novel approaches to NPs studies, it could help other scientists to employ them in their researches. The novel concept of the NPs-Pg correlation plot is still in its infancy and warrants more research for understanding its novelty. Moreover, it can also be used to develop NPs-Pg correlation plot of those NPs that enjoy a good quantity of literature.

Thus, ecofriendly synthesized Ru-cNMs could be capable of overcoming the aforementioned problems in an acceptable way. This review critically describes earlier publications made in this area and classifies them in an easy and in a perceptible manner. It aims to be a comprehensive, authoritative, critical, and accessible review of general interest in chemical science as it embodies all possible aspects of synthesis, characterization,

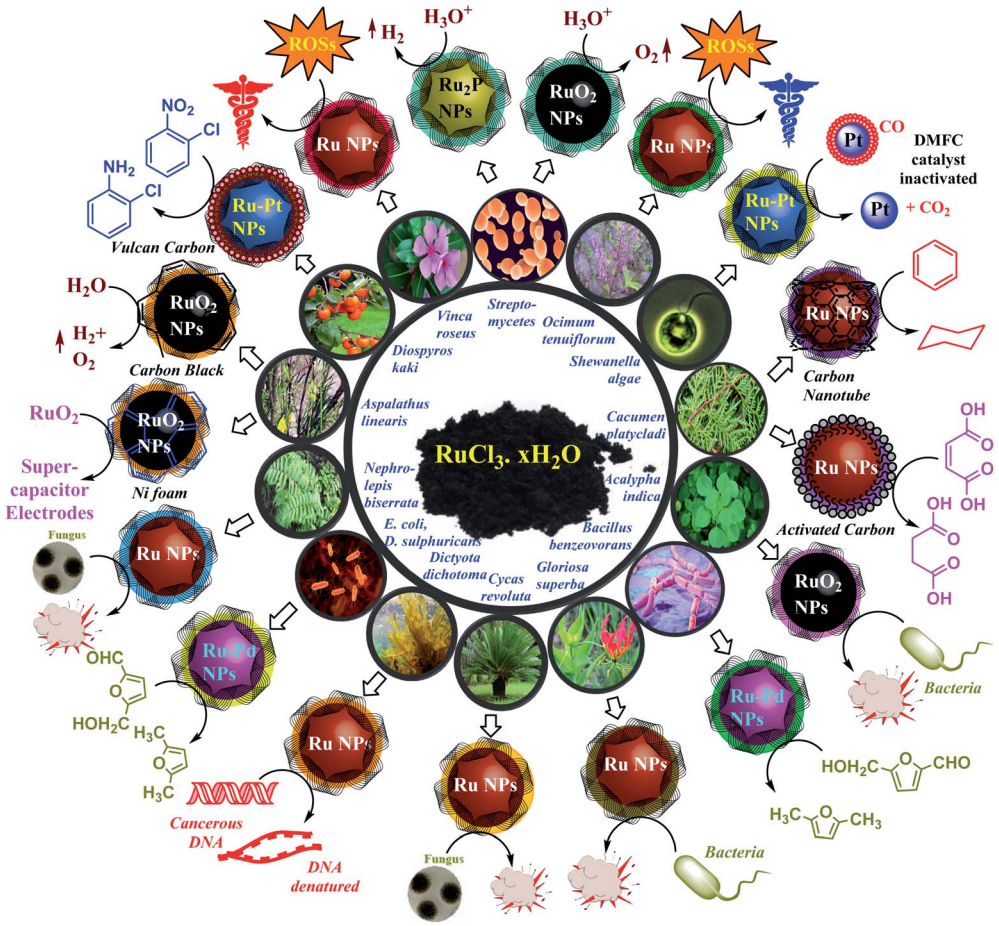

Scheme 1 Schematic representation of catalysis and bioactivity of Ru NMs.[7–11,19,45a,55,56,59,104]

and applications of Ru-cNMs and critically deals in a way to make them understandable for readers irrespective of their field of research. It attempts to cover all literature on this topic from 2003 to 2019. The review classifies these ecofriendly synthesized Ru-cNMs designed to date on the basis of their synthetic strategy. This facilitates critical discussions on their chemical, physical and biological properties and characterizations. Moreover, applications of these nanomaterials (NMs) have been described by classifying them on the basis of their bioactive and chemo-active nature. This review article also provides a critical comparison of Ag and Ru NPs due to the abundance of data available on Ag NPs as compared to Ru NPs. This would be certainly attractive to the readers of this review article. However, due to poor research data available in the area, this may be considered as a simplified review.

Green nanotechnology: the demand of the time

Nanotechnology is an ever-emerging field with wide-ranging applications. Synthetic approaches like top to bottom and bottom to top are easy, but employ toxic chemicals and develop high polydispersity. Green synthesis of metal NPs is a novel and ecofriendly solution to this problem.[12] Initial attempts paved the way to synthesize metal or metal oxide NPs using biological entities, starting from the most primitive (microscopic) to highly advanced (macroscopic) species.[13] Complex systems like living organisms undergo protoplasmic physiochemical reactions and evolve enzymatic redox reactions with their phylogenetic advancement.[14]

Plants are better candidates for the synthesis of metal NPs owing to their chemoregulation against heavy metal stresses *via* enzymatic or redox mechanisms. The inherent reductive physiology of these plants reduces unwanted peroxides, superoxides, and metal ions to metal-oxides and metal nanoclusters of lower oxidation states.[15] Stabilization of these nanoclusters is achieved through secondary metabolites such as flavonoids and terpenoids.[16] Initially, bacterial- or fungal-mediated NPs synthesis was avoided due to extensive sterilization and labour required, but recently they have turned out to be potent NP precursors or supports for catalytic activity.[17] Hence, various monometallic and bimetallic NPs, like bio RuPd, Ru_2P and RuO_2 NPs, have been prepared within dried bacterial or fungal biomass and are later ground with them so that biomass can facilitate catalysis and recovery. Ag and Au NPs have been extensively studied in the last few decades which has guided the synthesis of NPs of Cu, Ni, and Ru using similar protocols with minimum modifications.[18]

Moreover, the phenomenal synthesis and "Pd seeding" mechanism of core–shell AuPd NPs facilitated the synthesis of heterobimetallic Ru NPs.[19] Such strategies provided both quantitative and qualitative synthesis of metal NPs with significant yield, bioactivity, broad-spectrum catalytic activity, and efficient ligand transfer reactions.

Synthetic strategy and applications

Ruthenium (Ru) being a congener of the Fe group belongs to 4d series along with Ag. Being close to the Mn group it can show higher oxidation states and coordination numbers. Its catalytic properties are similar to those of Pt, Pd, and Ir complexes; still, it has been exploited more than these metals. This inclination towards Ru is due to its affordability, as Ru (1.48 $ per g) is cheaper than Pt (35 $ per g), Pd (19.4 $ per g), and Ir (17.6 $ per g).[20] Novel nanoclusters incorporating Ru in either form show enhanced catalytic efficiency. Reduction of Ru^{3+} ($RuCl_3 \cdot xH_2O$) to Ru^0 ($s^0\ d^5$ to $s^1\ d^7$) is energetically expensive as compared to the reduction of Ag^+ to Ag^0 ($s^0\ d^{10}$ to $s^1\ d^{10}$). Owing to the stabilization by ligand field, Ru^0 ($s^1\ d^7$, ligand field stabilization energy (LFSE): 18.0 Dq) experiences better capping as compared to the one offered for Ag^0 ($s^1\ d^{10}$, LFSE: 0.0 Dq). This can be proved through high-temperature, extract-mediated synthesis of Ru NPs.[21] Various plants, particularly *Catharanthus roseus*, *Nephrolepis biserrata*, *Cycas revoluta*, *Ocimum tenuiflorum*, *Diospyros kaki*, *Gloriosa superba*, *Aspalathus linearis*, *Cacumen platycladi*, and *Dictyota dichotoma*, are known for their significant reducing and antioxidant properties.[22] High-temperature treatment and bio extracts cause reduction of Ru^{3+}, followed by its facile stabilization *via* bioactive compounds. However, the oxidation of Ru^{+3} to Ru^{+4} ($s^0\ d^5$ to $s^0 d^4$) to synthesize RuO_2 NPs is found to be more facile than the synthesis of Ru and Ag NPs. Their stabilization ($s^0\ d^4$, LFSE: 4.0 Dq) is less than that of Ru NPs, and more than that of Ag NPs.[23] This again can be confirmed from the reported synthetic approaches for the synthesis of RuO_2 NPs. Their synthesis is very feasible and done under normal conditions. Infrared spectra confirm the presence of minute amounts of RuO_2 as a byproduct in Ru NPs' synthesis, owing to atmospheric oxidation. Calcination is done to control magnetic agglomeration of RuO_2 NPs owing to low stabilization.[24] During calcination, functional moieties denature to smaller molecular fragments enhancing the capability of these organic moieties to cap metal NPs.

RuO_2 being the hardest inorganic material can show selective conductivity under different physicochemical states. It exhibits electron–hole conductivity, in its hydrated and crystalline form, respectively.[25] Being equally durable and hard as diamond, its modulus is equivalent to that of the fluorite crystal lattice.[26] RuO_2 NPs when added to biodiesels improve their efficiency by maximising energy output and minimising pollutant efflux rate.[27] Owing to the wide-ranging applications of RuO_2 NPs, they have become expensive, but costs can be reduced by adopting greener synthetic strategies. Studies on chemically synthesized Ru and RuO_2 NPs have been done, involving direct methanol fuel cells (DMFCs), supercapacitor electrodes, chemiluminescence, anticancer activity, and degradation catalysis.[28] RuO_2 NPs are popular due to their redox properties and conductance.[29] The strong bioactivity of Ru attracts scientists to employ it in biological systems.[30] The physicochemical properties of Ru and RuO_2 NPs are well established, but their green synthesis, bioactivity and catalysis are at an early stage. Until 2012, there were no communications regarding them, but in the past eight years, some successful efforts have been made. As depicted in Scheme 2, green Ru-cNMs have been shown to have the ability to reduce aromatic compounds and functional groups, catalyze water splitting reactions (WSRs), reactivate DMFCs, and exhibit bioactivity such as antimicrobial, antioxidative and anticancer properties.

The present contribution reviews Ru-cNMs synthesized using bio-extracts. To the authors' best knowledge, no review could be traced for such a topic of immense interest. Syntheses proposed for Ru NPs employ bio-extracts that have already been used for Ag/Au NPs' synthesis so that an approximate idea of the bioactivity and particle size characterizations could be obtained.[31] The review aims to critically analyze the data available on initially developed Ru nano-systems and to be a guide for quality research work in this field. Emphasis has been given on making the text comprehensive and reader-friendly so to make it accessible, not only for the chemical community but also for scientists of diverse fields of studies.

Syntheses of Ru-cNMs have been done using chemical reductants like $NaBH_4$, which can be represented by the following ionic equation:

Reduction:

$$3BH_4^- + 8Ru^{3+} + 12H_2O \rightarrow 3B(OH)_4^- + 8Ru^0 + 24H^+$$

Capping:

$$nRu^0 + mS^{-x} \rightarrow [[Ru]_n - (S)_m]^{-yx}\ \{y_{max}: m\}$$

The charge over these NP surfaces depends on the ligand employed in the stabilization. However, bioreduction techniques are ecofriendly and employ bioreductants like cell biomass, cellular proteins, and secondary metabolites that are also capable of stabilizing the NMs. In addition to this, calcination being an optional strategy oxidizes the capping agents on the surface of NMs. These can be depicted in the following reaction:

reduction:

$$3(RR'H)C\text{–}OH + 2Ru^{3+} \rightarrow 3RR'C{=}O + 3H^+ + 2Ru^0$$

capping:

$$nRu^0 + mRR'C{=}O \rightarrow [[Ru]_n\text{–}(O{=}CRR')_m]\ \{\text{neutral pH}\}$$

$$nRu^0 + m(RR'H)C\text{–}O^- \rightarrow [[Ru]_n\text{–}(O\text{–}CRR')_m]^{-mx}\ \{\text{acidic pH}\}$$

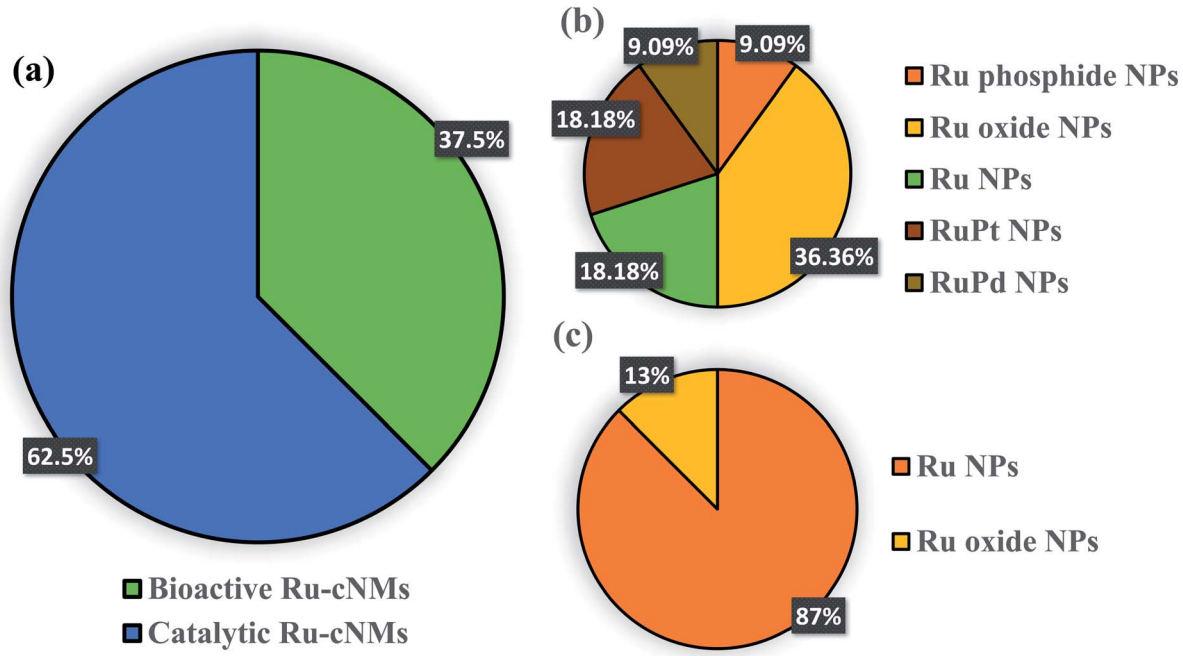

Scheme 2 Green Ru NMs synthesized since 2005, and their biological and catalytic applications. Bioactivity (blue) and catalysis (orange). (a) Major classification of Ru NMs based on the work done up to 2005. Sub-classification of (b) catalytic Ru NMs and (c) bioactive Ru NMs.

The capping agents may be either the reactant or the product generated. Moreover, efficiency of this supramolecular interaction may be modulated on the basis of spectator groups on substituents (R and R′ here). Apart from these, cell culture-mediated synthesis of Ru-cNMs is mostly enzymatic. These enzymes are active at incubation temperatures. Various synthetic strategies followed for synthesis of Ru-cNMs motivates us to classify these Ru-cNMs on the basis of reported synthetic strategies available.

Classification based on synthetic protocol

Metal NPs have been synthesized using two fundamental approaches, namely top-down and bottom-up. The top-down approach involves disintegration of bulk material to nanosized particles, and the bottom-up approach involves the aggregation of small-size materials to nanosized particles.[32] Various techniques have been proposed for the synthesis of Ru-cNMs, but the green synthetic approach has enabled scientists to provide cheaper and ecofriendly Ru-cNMs. Bioactive Ru-cNMs have been synthesized using extracts of medicinal plants and cell mass of bacteria adopting the bottom-up technique. Metallic reduction could be either enzymatic or biochemical, but in most cases the former dominates. The stabilization of corresponding structures has been achieved by secondary metabolites. The bioactivity of Ru-cNMs is owing solely to their stress-enduring and bioprotective nature. However, their catalytic property and recycling ability warrants maintenance of their surface activity employing a suitable substrate.

There could be two bottom-up strategies for the synthesis of catalytic metal-cNMs, namely sol–gel method and adsorption-reduction method. These methods differ in the sequence of reduction and substrate upload. In the sol–gel method, a metal solution is reduced to metal sol followed by its loading over a suitable substrate. In the adsorption-reduction technique, metal ions are incorporated over the substrate and then reduced by a suitable reducing agent. Reports suggest that metal NPs synthesized *via* the sol–gel technique are more active than those synthesized through the adsorption-reduction technique, as the former is capable of generating nano-catalysts of suitable particle size with high surface activity.[33]

As depicted in Scheme 3, the structures can broadly be classified as monometallic or bimetallic NPs. Monometallic NPs can further be subdivided into catalytic and bioactive NMs, based on the presence or absence of substrate adsorption. The substrate-coated Ru-cNMs have been synthesized in order to employ them for catalysis. These NMs have been synthesized using the sol–gel immobilization method. Synthetic approaches are concerned with the catalytic efficiency of Ru and RuO_2 NPs. These bio-extracts cut down synthetic steps owing to their composition containing both reducing and stabilizing agents.

Ru NPs could be synthesized using a bioextract-mediated reduction process, whereas that of RuO_2 NPs involves bio-reduction followed by calcination steps. Bioextract-mediated metal NP synthesis was employed, whereby bioextracts could reduce a metal ion to its zero-valent state and stabilize it preferably at the nanosize.[34] This bottom-up technique has been employed for the synthesis of Ag and Au NPs and significant results have been obtained.[35] Thus it prompted and justified the

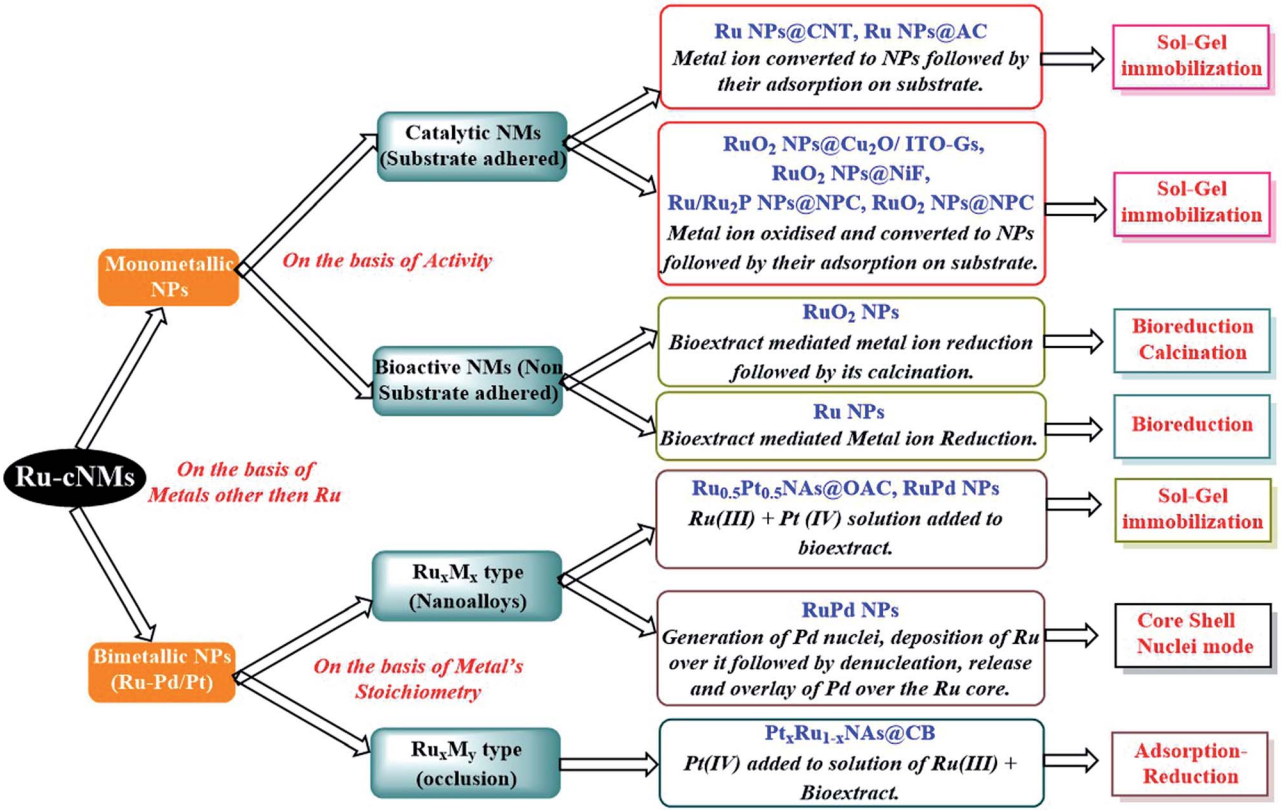

Scheme 3 Classification of various Ru NMs reported to date (2005–2019), on the basis of their synthesis strategy. Abbreviations: carbon nanotube (CNT), activated carbon (AC), oxidized activated carbon (OAC), carbon black (CB), nanoalloys (NAs), nickel foam (NiF), (N,P,C)-doped (NPC), indium tin oxide over glass substrate (ITO-Gs), doped over (@).[7–11,19,45a,55,56,59,104]

synthesis of Ru and RuO_2 NPs using extracts of medicinal plants.

Bimetallic NMs particularly Ru–Pt cNMs could be nanoalloys (Ru_xM_x) or bimetallic aggregations (Ru_xM_y where $y = 1 - x$ or multiples of x). The thermodynamic feasibility of Ru–Pt cNMs' synthesis has been confirmed by the formation enthalpy, −0.03 eV per atom, suggesting facile alloying of Ru–Pt cNMs from unalloyed counterparts. Apart from enhancement in catalytic activity, the addition of Pt(IV) to Ru(III) facilitates an easy reduction of Ru(III). It has been observed that by doping a substance of low reduction potential by a material of high reduction potential, the mixed potential becomes more positive leading to more facile reduction. Pt(IV), a metal of high reduction potential ($PtCl_6^{2-} + 4e \rightarrow Pt + 6Cl^-$; $E_{SCE} = 0.73$ V), when added to Ru(III), a metal of low reduction potential ($Ru^{3+} + 3e \rightarrow Ru$; $E_{SCE} = 0.30$ V), facilitates the reduction of Ru(III).[36]

The Ru_xM_x systems are synthesized by mixing metal ion solutions of Ru(III) and Pt(IV) in bio-extract, and Ru_xM_y systems are synthesized by mixing metal ion solutions like Pt(IV) in a solution of Ru(III) and bio-extract. These are modified sol–gel immobilization and adsorption-reduction techniques respectively. Hetero-bimetallic NMs have been employed for catalyzing cumbersome and unselective reactions. Bimetallic Ru–Pt NPs have been synthesized to catalytically reduce *o*-chloronitrobenzene to *o*-chloroaniline, a reaction of high commercial value but associated with multiple synthetic issues. Conventional reduction of nitro-aromatic systems is a tedious, high-temperature and time-consuming reaction. Moreover, substitution complicates the above process by dechlorinated side products.[37] Similarly, reactivation of CO-poisoned Pt catalysts in DMFCs by reducing CO is an energy-consuming and non-stoichiometric process.[38] As previously established, the sol–gel approach is synthetically much more efficient for nanoalloy synthesis as compared to the adsorption-reduction strategy.

The prominent synthesis of AuPd NPs *via* bacterial cell cultures has guided the synthesis of various core–shell hetero-bimetallic NPs like PdPt NPs and metal/non-metal core–shell NPs like Ru/RuO_2 NPs. This synthesis proved to be a boon in bacterial nanotechnology, such that green core–shell NPs synthesized so far have been synthesized through bacterial cell lines. Synthesis of RuPd NPs is quite similar to the synthesis of RuPt NPs, where Ru(III) solution is added to a mixture of Pd(II) salt and cell biomass. RuPd NCs (nanocatalysts) synthesized through metabolically active bacterial cell cultures (grown to mid-logarithmic phase) have been directly used for catalysis, without separating them from the cell biomass. Cell biomass of Gram-negative bacteria proved to be a better substrate for high catalytic efficiency, but a poor substrate for quantitative and qualitative synthesis. This could be attributed to the poly-hydroxy sugar groups present in endotoxin moieties of their cell coat that serve as excellent stabilizing agents. These endotoxin moieties arranged perpendicular to the cell coat surface could

also hinder the surface adherence of reagents, limiting efficient NPs-reagent interaction and generating by-products.[39] Bolivar *et al.* have reported that a higher concentration (nearly 4 times the wt% of Pd) of Ru gave core–shell RuPd NPs. But with equal concentration, separate monometallic NPs were obtained.

The synthesis of these core–shell NPs has been established through "Pd seeding" or "core–shell mode" mechanism as depicted in Scheme 4. An acidified solution of Pd(II) is added to the cell biomass for facile generation of free $PdCl_3^-$, *via* protonation of negatively charged protein residues. This intracellular Pd(II) is metabolically reduced to Pd(0) through hydrogenases. These grow further and are referred to as "Pd seeds". On the addition of Ru(III) solution, Pd seeds galvanically reduce Ru(III) to Ru(0) and get oxidized to Pd(II). The generated Pd(II) can either be collected (the catalytic activity of Pd(II) ions) or can be deposited back on Ru NPs by reducing back to Pd(0) through a reductant. Various reductants like ferrocene-hydroxylate, organoamine, and hydrogen gas have been used.

Reaction based on the above mechanism can be represented as:

$$\text{Lipid bilayer} + RuCl_3 + 2H^+ \rightarrow RuCl_2^- + HCl + H^+ \text{ lipid bilayer}$$

$$\text{Lipid bilayer} + PdCl_4^{2-} + 2H^+ \rightarrow PdCl_3^- + HCl + H^+ \text{ lipid bilayer}$$

$$2RuCl_2^- + nL \rightarrow RuL_n + 4Cl^-$$

$$H_2 + PdCl_3^- \rightarrow 2H^+ + Pd^0 \{\text{hydrogenases}\}$$

$$Pd^0 + RuL_n \rightarrow Pd^{2+} + Ru^0 + nL$$

$$xRu^0 \rightarrow (Ru)_x \{\text{Ru NPs}\}$$

$$Pd^{2+} + H_2 \text{ (reductant)} \rightarrow Pd^0 + 2H^+$$

$$\text{Side products: } RuL_n + Pd^0 \rightarrow Ru^{\delta-}Pd^{\delta+} \{\text{RuPd cluster}\}$$

$$wPd \rightarrow (Pd)_w \{\text{Pd NPs}\}$$

$$RuL_n + O_2 \rightarrow RuO_2 + nL \{RuO_2 \text{ NPs}\}$$

$$p[aPd^0 + kRu^0 + iRuO_2] \rightarrow [Pd_aO_bRu_c]_p \{\text{core–shell NPs}\}$$

{where $b = 2n$, $c = k + i$}

The organic biostabilizers containing –OH, $-NH_2$ groups may also behave as potent reductants. The generated RuPd core–shell NPs may also include indistinguishable patches of RuO_2 within Ru core adjacent to bimetallic junction, generated due to atmospheric oxidation of Ru(III). Several irregular dumbbell-shaped $Ru^{\delta+}Pd^{\delta-}$ composites may also be observed owing to the oxidation of Ru(III) through Pd(0). Ru NPs and Pd NPs were obtained as byproducts and could be separated by rigorous washings.[40]

Synthesis of these bimetallic Ru–Pt cNMs is done simply by adding stoichiometrically equal amounts of Ru(III) and Pt(IV) solution in bio-extracts. Sometimes, the reduction capability of bio-extracts could be enhanced by the addition of sodium formate.[41] The synthesis of Ru-cNMs revolves around four bottom-up synthesis strategies: sol–gel immobilization, adsorption–reduction, core–shell mode and bioreduction.

Characterization of Ru-cNMs

Ru^{3+} and its NPs (particle size < 10 nm) give characteristic absorption peaks at ~454 nm and ~430 nm respectively, used for monitoring their interconversion. Unlike Ru NPs,

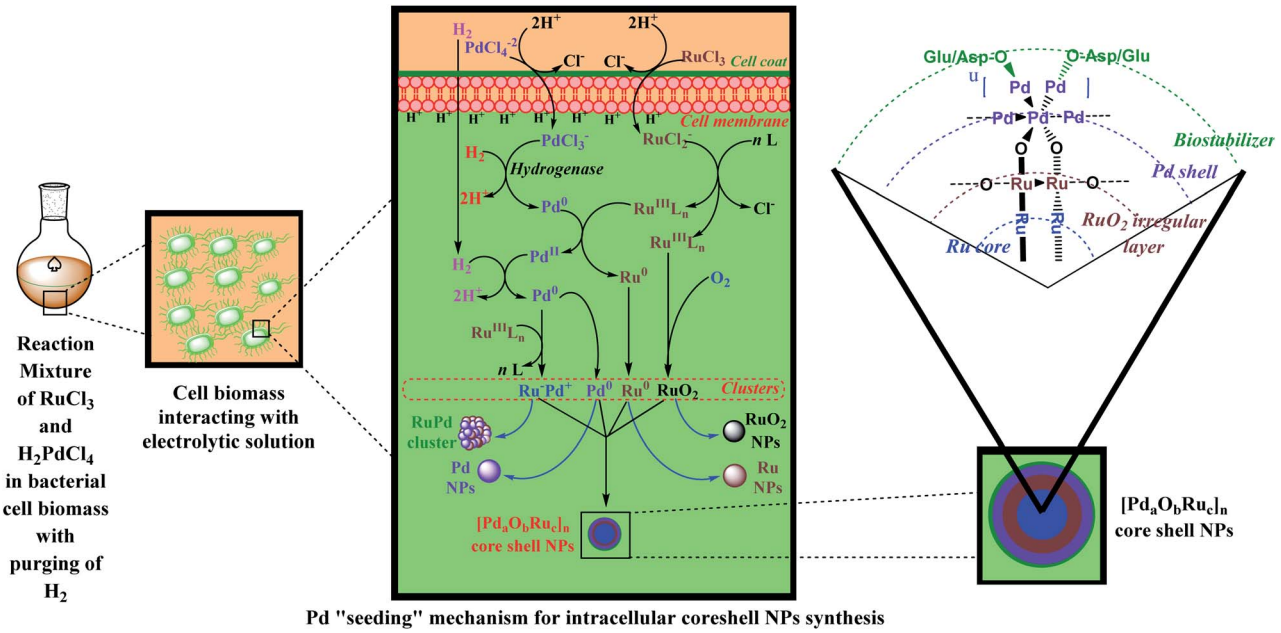

Scheme 4 Illustration depicting structure and "Pd seeding" mechanism for the synthesis of core–shell RuPd NPs as proposed by Deplanche *et al.*[19,104]

absorption spectra of Ru nanocolloids (particle size > 10 nm) have no signature peak and exhibit a Mie-type exponential decay pattern.[42] Spectral interferences are evident in methanolic extracts but not in aqueous extracts. The absorption band for RuO_2 NPs is found at ~428 nm, with some hypsochromic shift due to bioinorganic capping on the NP surface.[43] NPs cause quenching of phyto-fluorescence in either red or green or both regions due to nucleation and in turn stabilizes these NPs. This is evident from quenched emission from chlorophyll-functionalized Ru NPs. The serrated appearance of fluorescence spectra support biostabilization of Ru NPs.[44] Optical density of a vortexed solution of amorphous NPs is used to calculate optical band gap (E_g) and band tailing parameters of different photonic transitions using Tauc's relation and Tauc plots (ESI: SD3†) drawn for different transitions (*i.e.*, direct allowed, direct forbidden, indirect allowed and indirect forbidden transitions).[45] Allowed energy bandgap of RuO_2 NPs was deduced to be 2.1 eV, equivalent to the bandgap of Cu_2O used for WSR setup. Thus Ru-cNMs doped WSR setup was constructed and displayed efficient photocatalytic property (ESI: Fig. 1-a†).

The vibrational spectra of Ru NPs have been employed to identify functional moieties of stabilizers.[46] Owing to D_{4h} symmetry of RuO_2, its NPs exhibit 15 optical modes out of which A_{1g}, B_{2g}, E_g (strong) and B_{1g} (weak) modes are Raman active, and A_{2u} and E_u mode are IR active. Strong Raman active bands around 650, 710 and 530 cm^{-1} correspond to A_{1g}, B_{2g} and E_g modes respectively. A weak band corresponding to B_{1g} mode owing to bulk RuO_2 is also observed. IR spectra show two peaks corresponding to asymmetric A_{2u} and E_u stretching modes of RuO_2 at around 460 and 580 cm^{-1}. Green RuO_2 NPs show a hypsochromic shift in these bands due to the enhanced surface and stress effects. Support-coating RuO_2 NPs can be identified by an extra 1st harmonic A_{1g} Raman stretch owing to A_{1g} mode at around 1040 cm^{-1}.[47] Capping and reducing agents can be analyzed through dried samples of plant extracts before and after NP synthesis.[48] Dried KBr pellets of plant extracts showed a hypochromic shift in ν(C=C) and ν(O–H) vibrations. This is attributed to the binding of metal ions by flavonoids and reducing sugar. It has been reported that coating by polyvinylpropane stabilizes the structure most likely through C=O group formed by oxidation of C–OH group of bioextracts and consequently reducing the metal ions.[49]

Furthermore, the 3d core-level X-ray photon spectrum displays 2 peaks at 281.1 and 285.2 eV assigned to $3d_{5/2}$ and $3d_{3/2}$ spin–orbit components respectively. This supports the presence of Ru in RuO_2 NPs. The additional peak observed at 283.0 eV has been assigned to RuOH (ESI: Fig. 1-b†).[50] Additionally, the O 1s core level peak could be observed at 530 eV. The atomic surface concentration ratios calculated using (ESI: SD4†)

$$(C_O/C_{Ru}) = (A_O/S_O)/(A_{Ru}/S_{Ru})$$

(where C is the atomic surface concentration of the given species, A is absorption peak width for a particular species, and S is the sensitivity with respect to the orbitals of a particular atom) were reported for O 1s as $S_O = 2.93$ and for Ru $3d_{5/2}$ as $S_{Ru} = 7.39$.[51] This ratio for RuO_2 NPs increases as the surface-bound species varies from O_2 to H_2O.[52] Moreover, uncalcined Ru NPs show the C 1s peak at 285 eV, and support bio-capping of NPs but it overlaps with the $3d_{5/2}$ peak of Ru, hence interfering with the analysis of the 3d core spectrum.[53] In such cases, Ru is analyzed in the Ru 3p region, *i.e.*, peaks corresponding to $3p_{1/2}$ and $3p_{3/2}$ at around 485 and 460 nm.[54] Calcined RuO_2 NPs show both 3d and 3p core spectra with no spectral disturbances. Nitrogen moieties of biostabilizers show N 1s peaks at 398, 400 and 401 eV arising from pyridinic-N, pyrrolic-N, and graphitic-N respectively. However, Ru–P bonds of Ru_2P NPs show a doublet in the P 2p region at 130.0 eV and 130.7 eV.[55] In bimetallic NPs, peaks for another metal atom can also be detected. The $4f_{7/2}$ peak at 71.2 eV supports the presence of elemental Pt in RuPt nanoalloys. Minor atmospheric oxidation generates $3d_{5/2}$ peaks in Ru NPs owing to the presence of RuO_2. The deposition of these NPs on substrates like carbon nanotube (CNT) and Ni foam (NiF) may cause a peak shift of about 1–2.5 eV.[56] Bolivar *et al.* reported an increase of ν(C=O) and a decrease in ν(C–O) peak intensity which supports the formation of metal NPs *via* the bioreduction process as shown in Scheme 4. However, the observation of a small peak at ~535 eV supported the presence of adsorbed water over NPs. Its intensity decreases with a concomitant increase in metal concentration as adsorbed water may be exploited after capping of the metal NPs.[57]

The X-ray diffraction patterns of Ru NPs have been analyzed using broadcasted (sample coated on a film) samples.[58] However, there is no need of broadcasting if highly dispersed catalytic Ru-cNMs are used. Ru NPs doped over CNT and graphite displayed characteristic doublet at 42.3° and 25° respectively.[59] When these substrates are oxidized with nitric acid, some low-intensity peaks corresponding to the metallic phases can be identified. Particle size owing to ideal peak broadening can be deduced through the Debye–Scherrer formula.[60] However, surface-active Ru NPs synthesized from plant extracts are much smaller in size (<10 nm), owing to which they offer non-ideal peak broadening (ESI: Fig. 1-c†).[61] This strain-originated deviation can be deduced through Williamson Hall plots (ESI: SD5†).[62] RuO_2 NPs synthesized using *Acalypha indica*, calcined at 600 °C, had an orthorhombic lattice with some unidentified peaks owing to calcination-resistant impurities. However, uncalcined Ru NPs show various lattices like simple cubic, face-centred cubic, or hexagonal.[63] Band displacement and reduction of lattice parameters confirm the synthesis of bimetallic NPs.

X-ray absorption spectroscopy is a synchrotron radiation-based spectroscopy done to determine the local coordination number either in a monometallic or bimetallic metal cluster. Near-edge absorption spectra are used to analyze local bonding and other sensitive parameters of metal NPs (ESI: SD6†).[64] Bolivar *et al.* synthesized bio-derived RuPd bimetallic NPs, and calculated the local geometry, coordination number, composition and bond lengths. Core-shell RuPd NPs are composed of 30% Pd(0), 20% Pd(II), 3–5% Ru(0) and 45–47% Ru(IV). However, the geometry of the Ru centre remained undefined due to the

very similar atomic numbers of Ru and Pd and low concentration of Ru in RuPd NPs as depicted in Scheme 4.

EDAX spectra of broadcasted samples show an intense peak of Si owing to the glass matrix. Incomplete nucleation of bimetallic NPs results in a mismatch of metal composition in EDAX spectra (ESI: SD7†). Scanning and transmission electron micrographs are calibrated and analysed through image processing software, such as ImageJ.[65] STEM and HAADF proved to be helpful in determining the structure and hypothesising the composition of both high and low Ru concentration bio-derived RuPd NPs synthesized by Bolivar *et al.* Elemental mapping of low Ru concentration confirmed uniform distribution of Pd, surface enrichment of Ru, and intracellular deposition of Ru NPs. The core–shell structure of bio-derived RuPd NPs confirmed the Pd "seeding" mode of NP synthesis. However, minor availability of RuO_2 also confirmed the formation of $Ru^{\delta+}Pd^{\delta-}$ clusters, owing to the oxidative behaviour of Pd as depicted in Scheme 4.

Bioactivity of green Ru-cNMs is solely due to the bioactivity of bio-extracts employed for their synthesis. Turbidimetric assays, culture plate/zone of inhibition measurements and food poisoning assays have been performed for testing antimicrobial activity so that inhibitory concentrations can be measured.[66] The antioxidant properties of Ru-cNMs have been estimated by similar calculations through DPPH (2,2′-diphenyl-1-picrylhydrazyl-hydrate), ABTS (2,2′-azino-bis-3-ethylbenzothiazoline-6-sulfonate), superoxide radical scavenging (SORS), and hydroxyl radical scavenging (HRS) assays.[67] Anticancer activity of Ru NPs designed using *Dictyoma dichotoma* extracts was investigated by performing cytotoxicity studies with HeLa, MCF-7 and VERO cell lines and IC_{50} values and cell viability were graphically calculated through calibration plots of Ru NPs at 540 nm. In our recent publication (2019), we have put forward a novel idea of NPs-Pg correlation plots which correlate logarithmic value of NPs' size (R, nm) to the bioactivity index (b: inhibitory concentrations) arranged in phylogenetic order of plants used for synthesis. Advancement in phylogeny leads to the development of complex bioactive compounds that serve as better redox agents, stabilizing agents, or both (ESI: Fig. 2-a, b and c†). The enhancement of synthetic ability can generate NPs with much smaller size and high surface activity. Maxima and minima of biological index curve can reveal unknown plants with enhanced capability of NP synthesis. Theoretical particle size of such NPs can be graphically deduced. Exceptions can be classified as positive or negative deviations, broadening the scope of theoretical research in green nanochemistry. The crossover points produced due to these exceptions have special significance, as the two lines of the plot, corresponding to biological index and particle size, can now be correlated as $R = ke^b$; when $k = 1.00$, the logarithmic value of particle size will be equivalent to the bioactivity index and this point is called bioactivity-size equivalence. Hence, the plant candidate at that point will have an ability to supply a biological activity equal to logarithmic particle size. Such a plant can be called a bioactivity-size equivalence plant. These plots can act as a data bank, beneficial for selective synthesis of metal NPs.

Catalytic efficacy of metal NPs is expressed through their Brunauer–Emmett–Teller (BET) surface area and is estimated through N_2 physisorption.[68] BET surface area of biosynthesized water splitting Ru NPs was 12.5 times greater than that of commercially available Ru NPs (110 $m^2\ g^{-1}$). BET surface area of oxidized activated carbon substrate doped $Ru_{0.5}Pt_{0.5}$ NPs ($Ru_{0.5}Pt_{0.5}$ NPs@OAC) was in the range of 867 to 913 $m^2\ g^{-1}$, which is 6.3–6.7 times greater than that of Huang's NPs and 7.8–8.3 times higher than that of commercial Ru NPs. This is attributed to plant extract stabilization. Excessive loss of specific surface area is not acceptable for efficient catalysis and its estimation is used to deduce ambient doping concentration (ADC). Huang and his group adapted this strategy to deduce ADC and found it to be equal to 2% (w/w). Extensive doping decreased the specific surface area from 959 to 865 $m^2\ g^{-1}$ (ESI: SD8†).[69]

Electrochemical studies are done to establish HER (hydrogen evolution reaction), OER (oxygen evolution reaction) and supercapacitive properties of metal NPs. A standard electrochemical workstation consists of reference (Hg, Hg_2Cl_2/saturated KCl; $E^o = 0.24$ V), counter, and working electrodes dipped in 0.5 M H_2SO_4 or 2.0 M KOH, and buffered by lactic acid–NaOH or phosphate buffer. Working electrodes are prepared by coating a slurry of synthesized Ru-cNMs over glassy-carbon or ITO-glass substrate, and polarization curves are obtained.[70] Cyclic voltammetric (CV) studies reveal that RuO_2 NPs adhere to the substrate and change their surface area (ESI: Fig. 3-a and b†). This technique also leads to a semi-qualitative confirmation of NMs-substrate interaction and NPs' supercapacitive nature.[71]

Electrochemical impedance spectroscopy (EIS) reveals interfacial properties of metal-cNMs through Nyquist plots, prepared to illustrate an electronic equivalent circuit of established nano-electrochemical setup, using the Levenberg–Marquardt minimization process and ZsimpWin (ESI: Fig. 3-d†). Bioextract-mediated RuO_2 NPs show a Randles electronic equivalent circuit consisting of a combined series resistance (R_s) corresponding to the electrode's ionic resistance and active substance/collector interfacial resistance, and a parallel combination of charge transfer resistance (R_{ct}) and constant phase element (CPE).[72] Ru–Pt DMFC systems, proposed for preventing CO-mediated Pt inactivation, have been prepared and tested through an experimental DMFC setup. DMFC anodes and cathodes were continuously supplied by fuel (aqueous methanol) and ambient air. The open-circuit voltage between these electrodes is estimated as an indication of % Pt inactivation (ESI: SD9 and SD10†).

Ru-cNMs-based catalysis reported to date is *via* H_2-mediated reduction reactions. Hence, H_2 flow pressure is a deciding factor for catalysis. High-temperature TGA/DTA studies increased synthesis rate with poor selectivity; high temperature offers kinetic support to side reactions that are thermodynamically disfavoured (ESI: Fig. 6-b, c and f†). Calcined Ru-cNMs have high catalytic efficiency owing to the increased surface area on partial removal of excess plant biomass. However, calcination done at extremely high temperatures (>700 °C) leads to dislocation and crystal defects in catalysts reducing their

catalytic efficiency. Bimetallic Ru NPs have proved to be better catalysts as compared to monometallic ones. The amount of Pt and Ru to be consumed for preparing Ru–Pt cNMs shows a volcano profile, establishing that 1 : 1 ratio of Ru and Pt is highly catalytic. Although an increase in the aforementioned catalytic parameters offers high yield, more relevant high selectivity is obtained for slightly milder conditions.

Multifunctional nature of Ru-cNMs

Various reports of Ru and RuO_2 NPs have been communicated involving sophisticated protocols.[73] Some of the initial reports compared the properties of synthesized Ru NPs with those of other metal NPs.[74] Ru-cNMs have been exploited both as bioactive agents and as potent catalysts. However, studies done to date are concerned with either of them.[75] The immense applicability and affordability of these NPs have led to many patents. Mukherjee *et al.* (2003) were the first group to patent *Fusarium oxysporum* aqueous extract-mediated synthesis of Ru NPs, reporting their size to be around 5–100 nm. Deb *et al.* (2016) synthesized polydispersed Ru nano-fertilizers capable of transferring micro- and macronutrients to deficient plants, also patented. The first green Ru NPs have been extracellularly synthesized using *Pseudomonas aeruginosa* SM1, whereby Ru NPs at room temperature, without rigorous optimization, and their structural features were compared to Ag, Pd, Fe, Rh, Ni, Pt, Co, and Li NPs, synthesized through the same microbe.[76] NPs were supposed to be synthesized and capped through the action of primary and secondary amines and cells exhibited some "selective coat penetration" against Ru NPs. Recent studies reveal that, unlike other NPs, Ru NPs synthesized by this method are surface neutral inhibiting cell coat affinity and penetration. Recently, research groups have contributed to concluding a rough strategy for Ru and RuO_2 NP synthesis. The numerical data corresponding to each group are listed in ESI: SD1 and SD2.†

Metal NPs are well accepted by biological systems owing to the low oxidation state of the metal. A biostabilizer's multiple ligating ends are bioactive and promote critical aggregation up to surface-active range.[77] Moreover, these NPs can deliver phyto compounds to living systems and facilitate disease control.[78] In view of the anticancer property of Ag NPs synthesized from *Taxus baccata*, Ru NPs were also found interesting.[79] The bioactivity of NPs entirely depends on two aspects: selectivity of metal and nature of bioextracts. Heavy metals employed for synthesis may be either those that are biocompatible or those that can mimic metal ions found in biological systems. Ag and Au NPs belong to the first category for their well-known biocompatible nature.[80] Ru NPs come under the second category as they can mimic iron in biosystems.[81] Bioextract-originated bioactivity can arise only if bioextracts are of medicinal value. Plants like *Gloriosa superba*, *Catharanthus roseus*, *Ocimum tenuiflorum*, *Nephrolepis biserrata*, and *Cycas revoluta* have been used for the synthesis of Ru NPs. On the other hand, the synthesis of RuO_2 NPs has been carried out using *Acalypha indica* and *Aspalathus linearis*. Ru NPs have been synthesized by both aqueous and methanolic extracts.[82] The green synthesis of RuO_2 NPs is, however, limited to the employment of aqueous extract (ESI: SD1 and SD2†).

Bioactive Ru-cNMs

Gopinath *et al.* reported plant extract-mediated synthesis of Ru NPs using aqueous leaf extract of *Gloriosa superba*, a celebrated plant in Ayurvedic and Unani medicine, and established their significant bactericidal activity against Gram-positive bacteria.[83] Kannan *et al.* were, however, the first group to synthesize and establish the bioactivity of RuO_2 NPs obtained using aqueous leaf extract of *Acalypha indica.* These NPs have both adsorbed and adhered layers of water molecules followed by a carbonaceous layer, generating crystalline NPs and confirming the phase purity. Bioactivity was tested against Gram-positive and Gram-negative bacteria, showing a significant antibacterial activity of Ru NPs (ESI: SD1†). Antioxidants present in plants quench reactive oxygen species (ROS) which are considered to be a prime cause of ageing and cell death.[84] Plants have been exploited as natural antioxidants since time immemorial (ESI: SD1 and SD2†). Recently, we have synthesized Ru NPs using methanolic extracts of plants like *Nephrolepis biserrata* Furcans, *Cycas revoluta*, *Catharanthus roseus*, and *Ocimum tenuiflorum*. The basic reason for their selection lies in their well-known pharmaceutical properties.[85] Antifungal, DPPH, ABTS, SORS, and HSA assays showed a significant antifungal activity of Ru NPs synthesized using *Nephrolepis biserrata* and enhanced antioxidant properties of Ru NPs synthesized from *Catharanthus roseus*, *Nephrolepis biserrata* Furcans and *Ocimum sanctum*.

Anticancer activity of Ru NPs can be attributed to their enhanced affinity towards cancerous cells as compared to normal cells. Metal NPs apart from being surface active have the capability of releasing bioactive metal ions in biological systems. Moreover, their mode of action is twofold. Being similar to Fe, Ru binds more often to carcinogenic proteins. The anticancer activity of these Ru NPs may also be attributed to their ability to bind DNA by a mode similar to that of cisplatin.[86] Ru NPs mimic cisplatin in its irreversible binding of divalent metal complexes and NPs to N-bases that distort cancerous DNA.[87] The hard–soft acid–base principle confirms coordination of Ru(II) with N-bases (*i.e.*, from N(1,7) of adenine and guanine, N(3) of cytosine and deprotonated N(3) of uracil and thymine). Ru(II) mimics the anticancer activity of cisplatin and has an added advantage of its biocompatibility. Epigallactocatekin gallate-functionalized Ru NPs and gallic acid-functionalized Se/Ru nanoalloys showed efficient anticancer activity.[88] Apoptotic and MMP-2/MMP-9 protein inactivation mode of anticancer activity was proposed.[89] Ali *et al.* reported the synthesis and anticancer activity Ru NPs obtained using aqueous extract of a marine brown alga, *Dictyota dichotoma*. These NPs were challenged against HeLa, MCF-7, and VERO cell lines. The IC_{50} values were found equivalent to those of cisplatin (ESI: SD1 and SD2†). This idea guided the development of Ru(II) in biological systems.

Cancerous cells show high ROS activity with low pH, and Ru NPs with three-fold anticancer activity exploit these

characteristics for their activity. These monodispersed, surface-enhanced NPs are efficiently endocytosed and de-aggregated by hydrolytic lysosomes, releasing biostabilized Ru(0) clusters. These clusters interact with ROS (abundant in cancerous cells, and under a controlled level in normal cells owing to efficient activity of superoxide dismutases, NADH reductases and catalases) and channelize them into a thermodynamically feasible redox process where they are converted to biostabilized Ru(II) which further binds with cancerous DNA through hydroxy, carboxy or amine protons of biostabilizers. Ru NPs *via* this strategy could selectively target cancerous cell lines. This mechanism exploits higher concentrations of H^+ ions and ROS, in a spontaneous manner. Every such redox chain exhausts $2H^+$ ions and $2O_2^-$ species of the cancerous cells, hence showing both carcinocidal and carcinostatic mode of action as depicted in Scheme 5.[90]

Catalytic Ru-cNMs

Catalytic properties of Ru cNMs, as in WSR, hydrogenation, and fuel cells, have been investigated owing to their significant catalytic activity to serve as a clean and renewable fuel (ESI: SD1 and SD2†).[91] Metallic Ru and its phosphides, nitrides, and oxides used to catalyze the oxidation of water pose toxicity problems.[92] Hydrogenation reactions can develop better and safer fuels with high calorific value.[93] Various organometallic complexes have been proposed for this purpose, but their synthesis, selectivity and conversion efficiency remain unsatisfactory.[94] Applicability is enhanced if the same material could be recycled with a minimum loss of catalytic power. Metal NPs have been widely exploited for this purpose due to their surface activity. Liquid-phase hydrogenation of unsaturated compounds has also been done using Cu, Rh, Ir, Pd, and Ru catalysts.[95]

Ru photocatalysts available for WSR have a high energy requirement (>3 eV, ultraviolet region) hence presenting the need for a lower energy bandgap (within the visible region) required to split water. Doping of transition metal elements in semiconductor NPs offers high stability and quantum yield, and a complicated core–shell nanostructure, facilitating plasmonic excitations in the visible region (1.23 to 3 eV). The available bandgap of RuO_2 NPs ($E_g = 2.1$ eV) encouraged Banerjee *et al.* to employ a photoexcitable couple of RuO_2 NPs-Cu_2O semiconductor deposited over indium tin oxide and layered on a glass substrate (RuO_2 NPs-Cu_2O@ITO-GS; p-type, $E_{opt} = 2.54$ eV), as depicted in Scheme 6. Enhanced surface activity reduced the photoactivation energy facilitating e/h pair recombination and reduction of H^+ to H_2 and oxidation of $2O^{2-}$ to O_2.[96] Initial high rates of OER are attributed to adsorption/desorption of O^{2-} over Cu_2O surface.[97] These NPs were synthesized through solvent-assisted oxidation which is complicated, sensitive, and energetically demanding, encouraging scientists to investigate their bio-extract-mediated synthesis. Ismail *et al.* synthesized RuO_2 NPs using aqueous leaf extracts of *Aspalathus linearis via* aspalathin-mediated *o*-dihydroxy/*o*-benzoquinone redox reaction. Theoretical studies to establish their water-splitting action revealed a stoichiometric production of H_2 and O_2 after 227 h (ESI: SD1†).

Metal phosphides (of Cu, Ru, Ni) have been used for acidic HER but the high-temperature synthesis employing excess hypophosphides and red phosphorous releases poisonous phosphine gas.[98] This indicates an essential need of a simple

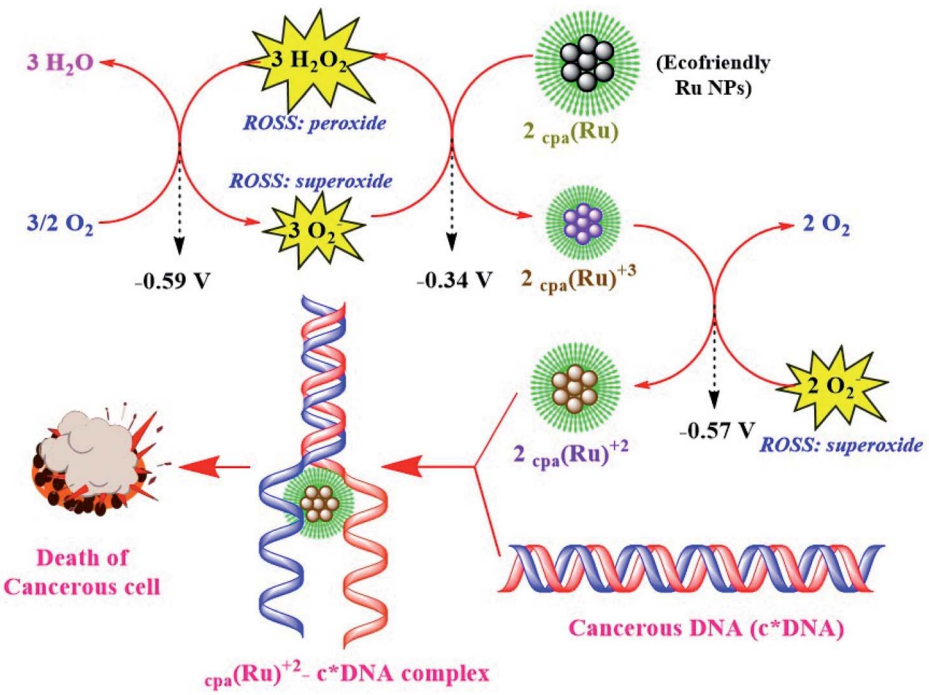

Scheme 5 Illustration depicting pathways of anticancer activity of Ru NPs.[87,88]

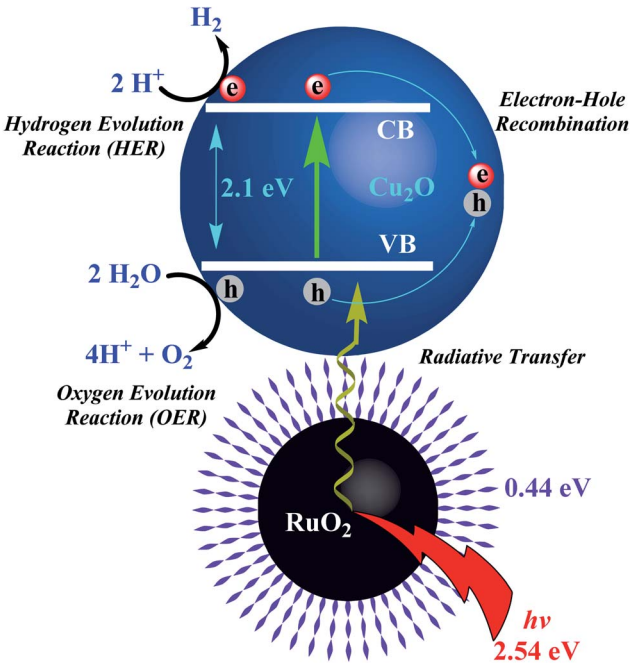

Scheme 6 Illustration depicting mechanism of hydrogen and oxygen evolution reactions (HER and OER) with RuO_2NPs-Cu_2O semiconductor.[97]

and safe protocol for metal phosphide NP synthesis. Ru-cNMs have been employed for the OER, as they were found capable of forming rigid O=O bonds.[99] RuO_2 NPs have been exploited for the OER owing to their small startup potential and significant stability, but tedious synthetic routes pose problems. Yu *et al.* proposed the synthesis of bi-phasic (hexagonal/orthorhombic) Ru/Ru_2P-cNMs doped over dried biomass (Ru/Ru_2P NPs@NPC) (ESI: SD1†) and yolk shelled RuO_2 NPs N/P dual-doped carbon template (RuO_2 NPs@NPC). HER activity was attributed to a surface Gibbs energy of 0.06 eV, pointing to easy adsorption/desorption of H^+/H_2. Biogenic reduction of Ru^{3+} was followed by partial phosphidation of Ru clusters owing bio-phosphorus moieties. Stability of RuO_2 NPs@NPC is less than that of Ru/Ru_2P NPs@NPC, as the former showed some degradation during the OER. Ru adhered over *Saccharomyces* cells was oxidized to a thick and dense layer of RuO_2, developing a quasi-vacuum environment and forming yolk–shell structure. When both of these materials were used as cathode and anode, *i.e.*,

$$\text{Ru/Ru}_2\text{P NPs@NPC (}-\text{) ll RuO}_2\text{NPs@NPC (+)}$$

they only needed 1.5 V to attain 10 mA cm^{-2}, with a durability of 83%, in 0.5 M H_2SO_4 electrolyte solution. This was much more efficient than the conventional 20% Pt/C (−) ll RuO_2 (+) electrolyzer.[100] The efficiency of this electrolyzer is 87.7% higher than that of solar WSR devices.[101]

Supercapacitive systems are energy storage devices with a long life cycle and high power density. These properties are exploited for power systems, memory storage systems, vehicle-assisting equipment, *etc.* Their suitable charging-discharging and supercapacitive nature provides a great advantage over normal batteries. Ismail *et al.* extended their work by employing their RuO_2 NPs decorated over NiF to develop supercapacitive electrodes (ESI: SD1†). This nanosystem was pseudocapacitive where faradaic charge transfer occurs at electrode–electrolyte interface with specific capacitance and energy density being much higher than those of capacitive systems. NPs had small particle size (5 nm) but were non-agglomerated, unlike the NPs reported by Kannan *et al.* Folds and cracks on NPs' surface were of electrochemical importance as they enhance the charging-discharging ability of NP electrodes, developing high specific capacitance and long cycling ability, *i.e.*, retaining only 97% of the capacitance after about 500 charge/discharge cycles, with efficient charge transfer through porous network of RuO_2 NPs decorated on NiF. As confirmed by CV and GCD studies over a potential range of 0.0–0.5 V, the RuO_2@NiF system was an efficient supercapacitor as compared to NiF, due to its adsorption-assisted, one-electron reversible reaction owing to intercalation of alkali metal ions. The specific capacitance decreases from 750 to 480 F g^{-1} with an increased current density from 10 to 100 A g^{-1}. EIS studies formulated an equivalent Randles circuit of this system with combined series resistance equal to 0.09 Ω in 0.2 M KOH solution, and near-capacitive nature of CPE component, owing to the introduction of ionic diffusion resistance.

Conventional hydrogenation catalysts of Cu, Ni, and Ru complexes decompose due to coke deposition during catalysis. Moreover, the generation of side products reduces quantitative yield and affects downstream processing. Catalytic hydrogenation of maleic acid to succinic acid produces compounds like butyrolactones, 1,4-butanediol, tetrahydrofuran, propionic acid, butyric acid and butanol as byproducts.[102] Development of side products and reactant decomposition are a threat to selectivity. Conversion of *o*-chloroaniline from *o*-chloronitrobenzene gives reduced yields due to unwanted dechlorination of reactant. Apart from other NPs, Ru NPs have been used for selective hydrogenation of D-glucose, xylose, α,β-unsaturated aldehydes and benzene.[103] However, these catalysts generate large amounts of heavy metal wastes due to their non-recyclable nature.

As depicted in Scheme 7, Ru and RuO_2 NPs synthesized from plant extracts gave better outputs and were energy conserving, non-hostile, and affordable. Huang *et al.* developed CNT coated with Ru NPs (Ru NPs@CNT) and activated carbon (AC) coated with Ru NCs (Ru NPs@AC) using aqueous leaf extracts of *Cacumen platycladi* for solid-state catalytic hydrogenation of benzene to cyclohexane and maleic acid to succinic acid, respectively. About 0.05 g of Ru NPs@CNT, at 80 °C and high pressure of N_2 gas, can give a 99.97% yield, within 0.5 h, for 6 cycles with negligible loss. Moreover, about 0.05 g of Ru NPs@AC, at 150 °C and high pressure of H_2 gas, can give 99.4% yield with 99.6% succinic acid selectivity in THF within, 0.5 h, for 5 cycles with negligible loss. The former was less efficient than later owing to the combined reduction–stabilization activity of plant extract. Other NCs developed by those authors for hydrogenation reaction were C-coated Ru nanoalloys (NAs) synthesized using aqueous extract of *Platycladus orientalis*,

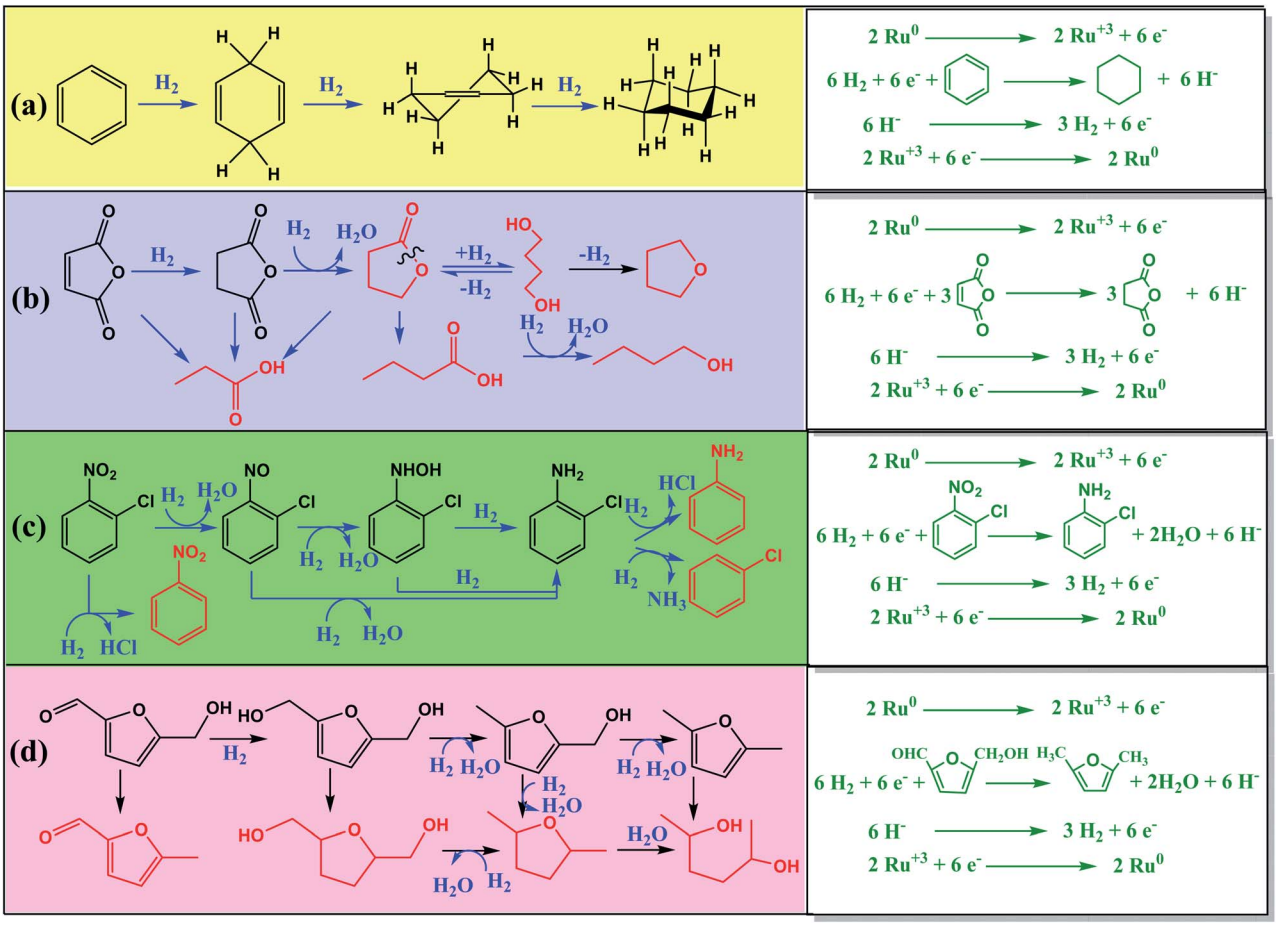

Scheme 7 Illustration depicting catalytic hydrogenation of organic compounds *via* catalytic Ru NMs.[11,56,59]

which they patented. Zhang *et al.* reported the synthesis of bimetallic ($Ru_{0.5}Pt_{0.5}$) NAs ($Ru_{0.5}Pt_{0.5}$NAs@OAC) using aqueous leaf extracts of *Diospyros kaki*, doped over HNO_3-oxidised activated carbon (OAC), for solid-state catalytic reduction of *o*-chloronitrobenzene to *o*-chloroaniline, a compound of immense industrial relevance but equally difficult to synthesize due to significant non-selectivity. Under inert conditions, 0.5 g of $Ru_{0.5}Pt_{0.5}$ NAs@OAC (Ru : Pt molar ratio of 1 : 1) using a high pressure of H_2 gas can give 99.8% conversion and 98.4% *o*-chloroaniline selectivity, within 45 min, for 5 cycles with equivalent efficiency (ESI: SD1†). The catalytic efficiency was found to be appealing due to better selectivity and higher conversion rate.

Oxidative degradation of cellulosic biowastes release furfural derivatives and 2,5-dimethylformamide (DMF) *via* intermediates like hydroxymethylformamide. The synthesis of bio-derived RuPd NPs was reported in 2019. Mikheenko *et al.*, Bolivar *et al.* and Omajali *et al.* have compared the synthesis of these NPs through Gram-negative (*E. coli*) and Gram-positive (*B. benzeovorans*) bacteria. Bolivar *et al.* compared the catalytic activity of bio-derived RuPd NPs on the basis of the concentration of Ru employed for the synthesis. The catalytic activities of high and low Ru concentration RuPd NPs were compared to that of commercial Ru NPs. The results were more promising for low Ru concentration bio-derived RuPd NPs as they could catalyze up-gradation of crude HMF to DMF with ~100% efficiency and 50% selectivity. These NPs were unable to surpass the catalytic activity of commercial Ru NPs.[104] Sano *et al.* synthesized bimetallic Ru–Pt NAs (Ru_xPt_{1-x}NAs@CB) using *Shewanella algae* tryptic soy broth culture and exploited them to prepare electrodes for inhibiting Pt inactivation due to CO, by oxidizing it to CO_2.[105] A mixture of sodium formate and bacterial extract was used as a reducing and stabilizing agent. In a DMFC, the anode is composed of a mixture of algal biomass, carbon black (CB) and NPs and the methanol passage is referred to as a cathode. CO inactivation and switch-off potential were investigated (ESI: SD1†). A fuel cell so prepared can provide energy from 3% (w/w) of methanol, and retain Pt activity, by giving a constant switch-off potential of 0.04 V after an initial inactivation period of 10 min, due to unalloyed sites of Pt.

Evaluation of green synthetic protocols

Paul Anastas defines green chemistry *as the utilization of a set of principles that reduces or eliminates the use or generation of hazardous substances in the design, manufacture and application of chemical products.* His book entitled "*Green Chemistry: Theory and Practice*" describes 12 principles of a green protocol that

Table 1 Synthetic protocols of Ru-cNMs and their critical analysis against 12 principles of green chemistry as stated by Paul Anastas

Name of synthetic protocol	Sol–gel immobilization	Adsorption-reduction	Bio-reduction	Core–shell synthesis
Number of reports for Ru-cNMs	8	1	6	3
Synthetic protocol	Metal solution is reduced to metal sol followed by its loading over a suitable substrate	Metal ions are incorporated over the substrate and then reduced by a suitable reducing agent	Metal electrolyte is reduced and stabilized by bioextracts, biomass, biologically derived compounds	*In vitro* synthesized metal particles reduce the metal ions, using reductive physiology of a live cell
Reducing agent (bioextract)	Reducing metabolites	Reducing metabolites	Reducing metabolites	Enzymatic reduction
Capping agent (bioextract)	Secondary metabolites	Secondary metabolites	Secondary metabolites	Protein residue
Solvent medium	Aqueous	Aqueous	Aqueous/non-aqueous	Aqueous
Energy consumption	Temperature, stirring	Temperature, stirring	Calcination may/may not	Incubation
Substrate employed	CNT, AC, ITO-Gs, NiF, biomass	CB	—	—
Activity of Ru-cNMs	High surface activity	Low surface activity	Catalysis and bioactivity	Catalysis
Principles of green protocol:				
(1) *Prevention*	👍	👍	👍	👍
(2) *Atom economy*	👍	👍	👍	👎
(3) *Less hazardous chemical synthesis*	👎	👍	👍	👍
(4) *Designing safer chemicals*	👎	👍	👍	👍
(5) *Safer solvents*	👍	👍	👍	👍
(6) *Design for energy efficiency*	👍	👍	👍	👎
(7) *Use of renewable feedstocks*	👎	👍	👍	👍
(8) *Reduce derivatives*	👍	👍	👍	👎
(9) *Catalysis*	👍	👍	👍	👍
(10) *Design for degradation*	👎	👎	👎	👎
(11) *Real-time analysis for pollution prevention*	👎	👎	👍	👎
(12) *Inherently safer chemistry for accident prevention*	👍	👍	👍	👍
Number of principles followed	7	**10**	**11**	7

are: prevention, atom economy, hazardous-free chemical synthesis, design of safer chemicals, use of safer solvents, design for energy efficiency, use of renewable feedstock, reduce derivatives, catalysis, design for degradation, real-time analysis for pollution prevention, and inherently safer chemistry for accident prevention.[106]

The present review mentions different protocols that have been exploited for synthesis of Ru-cNMs. Different green synthetic protocols have to be critically analysed in order to test

their validity against established principles. Table 1 compares various protocols on the basis of the above mentioned 12 principles of green chemistry. The nano-concentration of heavy metals in NMs decreases the risks of toxicity. Solvents used in the synthesis of Ru-cNMs are air-dried in order to collect the NMs. Hence employment of methanol or water may not imply any physical hazard to living organisms. The cell culture-mediated synthesis of core–shell NPs has high energy requirements, generates more byproducts and poses problems of waste generation. Substrates composed of heavy metals and non-biodegradable materials pose problems of pollution. However, some limitations like non-degradability are yet to overcome.

Conclusions

Three major challenges of the modern world are cancer, energy resources and pollution. Scientists have been working on these issues for many years. Most of the materials synthesized to date involved one or more of the three above mentioned threats at some point during application. We may obtain catalytic efficiency but with the dumping of toxic chemicals and heavy metals we are polluting water and air. Ru- and RuO_2-cNMs have a wide range of biochemical activity. When greener modes of synthesis are employed to synthesize these NPs, and when they are exploited to address the above issues, the need for such a material is fulfilled. Hence plant extract-mediated Ru-cNMs being employed in WSR, DMFCs, supercapacitive systems, anticancer systems, and catalytic systems have been able to tackle the regularly depleting resources, tackling cancer and establishing an ecofriendly way to realize all these efficiently. This novel field has much to explore and is capable of giving much more to human civilization. Strategies such as NPs-Pg plots establish theoretical applicability, along with efficient predictability. Employment of such nanosystems allows us to move towards a greener and ecofriendly way of applying chemistry. The present review is thus an embodiment of materials needed to meet modern challenges and encourages the present generation to be ready for taking up such problems in their future research studies.

Conflicts of interest

There are no conflicts to declare.

Acknowledgements

We are grateful to the Department of Chemistry, Institute of Science, Banaras Hindu University (I.Sc., BHU) and to Prof. K. George Thomas, Indian Institute for Scientific Education and Research, Thiruvananthapuram (IISER-TVM) for network support. We are also grateful to authors for their work in this field and for permission to use their figures.

Notes and references

1 V. D. Krishna, K. Wu, D. Su, M. C. J. Cheeran, J.-P. Wang and A. Perez, *Food Microbiol.*, 2018, **75**, 47–54.

2 J. L. Gardea-Torresdey, E. Gomez, J. R. Peralta-Videa, J. G. Parsons, H. Troiani and M. Jose-Yacaman, *Langmuir*, 2003, **19**, 1357–1361.

3 S. Naraginti, N. Tiwari and A. Sivakumar, *IOP Conf. Ser.: Mater. Sci. Eng.*, 2017, **263**, 022009.

4 T. Lazarević, A. Rilak and Ž. D. Bugarčić, *Eur. J. Med. Chem.*, 2017, **142**, 8–31.

5 J.-X. Gao, T. Ikariya and R. Noyori, *Organometallics*, 1996, **15**, 1087–1089.

6 M. N. Alam, N. Roy, D. Mandal and N. A. Begum, *RSC Adv.*, 2013, **3**, 11935–11956.

7 S. K. Srivastava and M. Constanti, *J. Nanopart. Res.*, 2012, **14**, 831.

8 (*a*) K. Gopinath, V. Karthika, S. Gowri, V. Senthilkumar, S. Kumaresan and A. Arumugam, *J. Nanostruct. Chem.*, 2014, **4**, 83; (*b*) S. K. Kannan and M. Sundrarajan, *Adv. Powder Technol.*, 2015, **26**, 1505–1511; (*c*) M. Syed Ali, V. Anuradha, R. Abishek, Y. Nagarajan and H. Sheeba, *NanoWorld J.*, 2017, **3**, 66–71.

9 P. K. Gupta, K. V. S. Ranganath, N. K. Dubey and L. Mishra, *Curr. Sci.*, 2019, **117**, 1308–1317.

10 E. Ismail, S. Khamlich, M. Dhlamini and M. Maaza, *RSC Adv.*, 2016, **6**, 86843–86850.

11 N. Sano, Y. Nakanishi, K. Sugiura, H. Yamanaka, H. Tamon, N. Saito and Y. Konishi, *J. Chem. Eng. Jpn.*, 2016, **49**, 488–492.

12 T. Garland, A. F. Bennett and E. L. Rezende, *J. Exp. Biol.*, 2005, **208**, 3015–3035.

13 P. Sharma, A. B. Jha, R. S. Dubey and M. Pessarakli, *J. Bot.*, 2012, **2012**, 26.

14 B. C. Tripathy and R. Oelmüller, *Plant Signal. Behav.*, 2012, **7**, 1621–1633.

15 (*a*) I. Morkunas, A. Woźniak, V. C. Mai, R. Rucińska-Sobkowiak and P. Jeandet, *Molecules*, 2018, **23**, 2320; (*b*) S. Jain and M. S. Mehata, *Sci. Rep.*, 2017, **7**, 15867; (*c*) J. Mittal, A. Batra, A. Singh and M. M. Sharma, *Adv. Nat. Sci.: Nanosci. Nanotechnol.*, 2014, **5**, 043002.

16 (*a*) S. Iravani, *Int. Scholarly Res. Not.*, 2014, **2014**, 18; (*b*) Z.-Y. Wu, B.-C. Hu, P. Wu, H.-W. Liang, Z.-L. Yu, Y. Lin, Y.-R. Zheng, Z. Li and S.-H. Yu, *NPG Asia Mater.*, 2016, **8**, e288.

17 (*a*) P. Elia, R. Zach, S. Hazan, S. Kolusheva, Z. e. Porat and Y. Zeiri, *Int. J. Nanomed.*, 2014, **9**, 4007–4021; (*b*) I.-M. Chung, A. Abdul Rahuman, S. Marimuthu, A. V. Kirthi, K. Anbarasan, P. Padmini and G. Rajakumar, *Exp. Ther. Med.*, 2017, **14**, 18–24.

18 (*a*) C. J. Pandian, R. Palanivel and S. Dhananasekaran, *Chin. J. Chem. Eng.*, 2015, **23**, 1307–1315; (*b*) Y. Zhang, H. Jiang, Y. Wang and M. Zhang, *Ind. Eng. Chem. Res.*, 2014, **53**, 6380–6387.

19 (*a*) J. B. Omajali, J. Gomez-Bolivar, I. P. Mikheenko, S. Sharma, B. Kayode, B. Al-Duri, D. Banerjee, M. Walker, M. L. Merroun and L. E. Macaskie, *Sci. Rep.*, 2019, **9**, 4715; (*b*) J. Gomez-Bolivar, I. P. Mikheenko, R. L. Orozco, S. Sharma, D. Banerjee, M. Walker, R. A. Hand, M. L. Merroun and L. E. Macaskie, *Sci. Rep.*, 2019, **10**, 1276.

20 G. Viau, R. Brayner, L. Poul, N. Chakroune, E. Lacaze, F. Fiévet-Vincent and F. Fiévet, *Chem. Mater.*, 2003, **15**, 486–494.
21 R. J. Deeth, in *Comprehensive Coordination Chemistry II*, ed. J. A. McCleverty and T. J. Meyer, Pergamon, Oxford, 2003, pp. 439–442.
22 (*a*) A. Nisar, A. Mamat, M. I. H. Mohamed Dzahir, M. Aslam and M. S. Ahmad, *Antioxidant and Total Phenolic Content of Catharanthus roseus Using Deep Eutectic Solvent*, 2017; (*b*) F. A. Manan, D. D. Mamat, A. A. Samad, Y. S. Ong, K. F. Ooh and T.-T. Chai, *Global NEST J.*, 2015, **3**, 544–554; (*c*) A. Moawad, M. Hetta, J. K. Zjawiony, M. R. Jacob, M. Hifnawy, J. P. J. Marais and D. Ferreira, *Planta Med.*, 2010, **76**, 796–802; (*d*) F. L. Hakkim, C. G. Shankar and S. Girija, *J. Agric. Food Chem.*, 2007, **55**, 9109–9117; (*e*) A. Hossain, H. K. Moon and J.-K. Kim, *Food Sci. Biotechnol.*, 2018, **27**, 177–184; (*f*) S. Jana and G. S. Shekhawat, *Fitoterapia*, 2011, **82**, 293–301; (*g*) E.-J. Lee and H.-D. Jang, *BioFactors*, 2004, **21**, 285–292; (*h*) D.-P. Xu, Y. Li, X. Meng, T. Zhou, Y. Zhou, J. Zheng, J.-J. Zhang and H.-B. Li, *Int. J. Mol. Sci.*, 2017, **18**, 96; (*i*) S. Tejada and A. Sureda, *J. Coast. Life Med.*, 2014, **2**(5), 362–366.
23 R. J. Deeth, in *Comprehensive Coordination Chemistry II*, ed. J. A. McCleverty and T. J. Meyer, Pergamon, Oxford, 2003, pp. 643–650.
24 T. Liu, B. Feng, X. Wu, Y. Niu, W. Hu and C. M. Li, *ACS Appl. Energy Mater.*, 2018, **1**, 3143–3150.
25 Y. Lin, N. Zhao, W. Nie and X. Ji, *J. Phys. Chem. C*, 2008, **112**, 16219–16224.
26 J. S. Tse, D. D. Klug, K. Uehara, Z. Q. Li, J. Haines and J. M. Léger, *Phys. Rev. B: Condens. Matter Mater. Phys.*, 2000, **61**, 10029–10034.
27 J. Arunprasad and T. Elango, *Energy Sources, Part A: Recovery, Utilization, and Environmental Effects*, 2019.
28 (*a*) D. R. Rolison, P. L. Hagans, K. E. Swider and J. W. Long, *Langmuir*, 1999, **15**, 774–779; (*b*) W. Wang, S. Guo, I. Lee, K. Ahmed, J. Zhong, Z. Favors, F. Zaera, M. Ozkan and C. S. Ozkan, *Sci. Rep.*, 2014, **4**, 4452; (*c*) L. Zhang and S. Dong, *Anal. Chem.*, 2006, **78**, 5119–5123; (*d*) Y. Zhou, Q. Yu, X. Qin, D. Bhavsar, L. Yang, Q. Chen, W. Zheng, L. Chen and J. Liu, *ACS Appl. Mater. Interfaces*, 2016, **8**, 15000–15012; (*e*) P. Ganji and P. W. N. M. van Leeuwen, *J. Org. Chem.*, 2017, **82**, 1768–1774; (*f*) A. Sahoo and S. Patra, *ACS Appl. Nano Mater.*, 2018, **1**, 5169–5178.
29 (*a*) D. P. V. Kumar, A. Ramdass and S. Rajagopal, *Ruthenium Nanocatalysis on Redox Reactions*, 2013; (*b*) M. Zafar, M. Tausif, Z. Haq, M. Ashraf and S. Hussain, *New Development of Anodic Electro-catalyst for Chlor-alkali Industry*, 2016.
30 A. Roy, O. Bulut, S. Some, A. K. Mandal and M. D. Yilmaz, *RSC Adv.*, 2019, **9**, 2673–2702.
31 G. Zhan, M. Du, J. Huang and Q. Li, *Catal. Commun.*, 2011, **12**, 830–833.
32 O. V. Kharissova, H. V. R. Dias, B. I. Kharisov, B. O. Pérez and V. M. J. Pérez, *Trends Biotechnol.*, 2013, **31**, 240–248.
33 H. K. Sadhanala, V. K. Harika, T. R. Penki, D. Aurbach and A. Gedanken, *ChemCatChem*, 2019, **11**, 1495–1502.
34 Y. Yulizar, T. Utari, H. A. Ariyanta and D. Maulina, *Journal of Containing nanomaterials*, 2017, **2017**, 6.
35 R. Ahmad and A. Mirza, *Global Journal of nanomedicine*, 2017, **2**(3), 1–2.
36 G. Sharma, A. Kumar, S. Sharma, M. Naushad, R. Prakash Dwivedi, Z. A. Alothman and G. T. Mola, *J. King Saud Univ., Sci.*, 2019, **31**, 257–269.
37 H. K. Kadam and S. G. Tilve, *RSC Adv.*, 2015, **5**, 83391–83407.
38 P. Joghee, J. N. Malik, S. Pylypenko and R. O'Hayre, *MRS Energy & Sustainability*, 2015, **2**, E3.
39 K. N. Thakkar, S. S. Mhatre and R. Y. Parikh, *Nanomed. Nanotechnol. Biol. Med.*, 2010, **6**, 257–262.
40 K. Deplanche, M. L. Merroun, M. Casadesus, D. T. Tran, I. P. Mikheenko, J. A. Bennett, J. Zhu, I. P. Jones, G. A. Attard, J. Wood, S. Selenska-Pobell and L. E. Makaskie, *J. R. Soc. Interface*, 2012, **9**, 1705–1712.
41 M. Nasrollahzadeh, S. M. Sajadi and A. Hatamifard, *J. Colloid Interface Sci.*, 2015, **460**, 146–153.
42 W. Chen, D. Ghosh, J. Sun, M. C. Tong, F. Deng and S. Chen, *Electrochim. Acta*, 2007, **53**, 1150–1156.
43 (*a*) V. D. Patake and C. D. Lokhande, *Appl. Surf. Sci.*, 2008, **254**, 2820–2824; (*b*) R. G. Haverkamp and A. T. Marshall, *J. Nanopart. Res.*, 2009, **11**, 1453–1463.
44 (*a*) S. M. Ng, M. Koneswaran and R. Narayanaswamy, *RSC Adv.*, 2016, **6**, 21624–21661; (*b*) U. K. Parashar, V. Kumar, T. Bera, P. S. Saxena, G. Nath, S. K. Srivastava, R. Giri and A. Srivastava, *Nanotechnology*, 2011, **22**, 415104.
45 (*a*) E. Ismail, A. Diallo, M. Khenfouch, S. M. Dhlamini and M. Maaza, *J. Alloys Compd.*, 2016, **662**, 283–289; (*b*) A. S. Hassanien and A. A. Akl, *J. Alloys Compd.*, 2015, **648**, 280–290; (*c*) S. Sirohi and T. P. Sharma, *Opt. Mater.*, 1999, **13**, 267–269.
46 (*a*) E. Saion, E. Gharibshahi and K. Naghavi, *Int. J. Mol. Sci.*, 2013, **14**, 7880–7896; (*b*) T. P. Luxton, M. J. Eick and K. G. Scheckel, *J. Colloid Interface Sci.*, 2011, **359**, 30–39.
47 (*a*) J. G. Kay, D. W. Green, K. Duca and G. L. Zimmerman, *J. Mol. Spectrosc.*, 1989, **138**, 49–61; (*b*) Y.-T. Kim, K. Tadai and T. Mitani, *J. Mater. Chem.*, 2005, **15**, 4914–4921.
48 (*a*) S. S. Shankar, A. Ahmad and M. Sastry, *Biotechnol. Prog.*, 2003, **19**, 1627–1631; (*b*) G. Zhang, M. Du, Q. Li, X. Li, J. Huang, X. Jiang and D. Sun, *RSC Adv.*, 2013, **3**, 1878–1884.
49 J. Huang, L. Lin, D. Sun, H. Chen, D. Yang and Q. Li, *Chem. Soc. Rev.*, 2015, **44**, 6330–6374.
50 A. Nemamcha, J.-L. Rehspringer and D. Khatmi, *J. Phys. Chem. B*, 2006, **110**, 383–387.
51 R. Fu, Z. Ma and J. P. Zheng, *J. Phys. Chem. B*, 2002, **106**, 3592–3596.
52 D. Rochefort, P. Dabo, D. Guay and P. M. A. Sherwood, *Electrochim. Acta*, 2003, **48**, 4245–4252.
53 H. J. Lewerenz, S. Stucki and R. Kötz, *Surf. Sci.*, 1983, **126**, 463–468.
54 D. Briggs, *Surf. Interface Anal.*, 1981, **3**(4), 1.
55 J. Yu, G. Li, H. Liu, L. Zhao, A. Wang, Z. Liu, H. Li, H. Liu, Y. Hu and W. Zhou, *Adv. Funct. Mater.*, 2019, **29**, 1901154.

56 Z. Zhang, Y. Suo, J. He, G. Li, G. Hu and Y. Zheng, *Ind. Eng. Chem. Res.*, 2016, **55**, 7061–7068.
57 J. Baltrusaitis, B. Mendoza-Sanchez, V. Fernandez, R. Veenstra, N. Dukstiene, A. Roberts and N. Fairley, *Appl. Surf. Sci.*, 2015, **326**, 151–161.
58 S. Ponarulselvam, C. Panneerselvam, K. Murugan, N. Aarthi, K. Kalimuthu and S. Thangamani, *Asian Pac. J. Trop. Biomed.*, 2012, **2**, 574–580.
59 (*a*) Y. Ma, Y. Huang, Y. Cheng, L. Wang and X. Li, *Appl. Catal., A*, 2014, **484**, 154–160; (*b*) Y. Huang, Y. Ma, Y. Cheng, L. Wang and X. Li, *Appl. Catal., A*, 2015, **495**, 124–130.
60 U. Holzwarth and N. Gibson, *Nat. Nanotechnol.*, 2011, **6**, 534.
61 Y. Zhao and J. Zhang, *J. Appl. Crystallogr.*, 2008, **41**, 1095–1108.
62 (*a*) A. Khorsand Zak, W. H. A. Majid, M. E. Abrishami and R. Yousefi, *Solid State Sci.*, 2011, **13**, 251–256; (*b*) V. D. Mote, Y. Purushotham and B. N. Dole, *Journal of Theoretical and Applied Physics*, 2012, **6**, 6.
63 I. Zhitomirsky, *Mater. Lett.*, 1998, **33**, 305–310.
64 M. Borowski, *J. Phys. IV*, 1997, **7**(2), 259–260.
65 M. Vippola, M. Valkonen, E. Sarlin, M. Honkanen and H. Huttunen, *Nanoscale Res. Lett.*, 2016, **11**, 169.
66 J. Gopal, S. Chun, V. Anthonydhason, S. Jung, B. N. Mwang'ombe, M. Muthu and I. Sivanesan, *J. Cluster Sci.*, 2018, **29**, 207–213.
67 (*a*) S. B. Kedare and R. P. Singh, *J. Food Sci. Technol.*, 2011, **48**, 412–422; (*b*) R. Re, N. Pellegrini, A. Proteggente, A. Pannala, M. Yang and C. Rice-Evans, *Free Radicals Biol. Med.*, 1999, **26**, 1231–1237; (*c*) B. Hazra, S. Biswas and N. Mandal, *BMC Complementary Altern. Med.*, 2008, **8**, 63; (*d*) C. Thomas, M. M. Mackey, A. A. Diaz and D. P. Cox, *Redox Rep.*, 2009, **14**, 102–108.
68 M. Zhou, Z. Wei, H. Qiao, L. Zhu, H. Yang and T. Xia, *Journal of Containing nanomaterials*, 2009, **2009**, 5.
69 (*a*) K. S. Walton and R. Q. Snurr, *J. Am. Chem. Soc.*, 2007, **129**, 8552–8556; (*b*) D. A. Gómez-Gualdrón, P. Z. Moghadam, J. T. Hupp, O. K. Farha and R. Q. Snurr, *J. Am. Chem. Soc.*, 2016, **138**, 215–224; (*c*) M. Du, G. Zhan, X. Yang, H. Wang, W. Lin, Y. Zhou, J. Zhu, L. Lin, J. Huang, D. Sun, L. Jia and Q. Li, *J. Catal.*, 2011, **283**, 192–201.
70 N. G. García-Peña, R. Redón, A. Herrera-Gomez, A. L. Fernández-Osorio, M. Bravo-Sanchez and G. Gomez-Sosa, *Appl. Surf. Sci.*, 2015, **340**, 25–34.
71 W.-C. Chen, C.-C. Hu, C.-C. Wang and C.-K. Min, *J. Power Sources*, 2004, **125**, 292–298.
72 J.-K. Lee, H. M. Pathan, K.-D. Jung and O.-S. Joo, *J. Power Sources*, 2006, **159**, 1527–1531.
73 (*a*) F. Z. Amir, V. H. Pham and J. H. Dickerson, *RSC Adv.*, 2015, **5**, 67638–67645; (*b*) R. Marcos Esteban, K. Schütte, D. Marquardt, J. Barthel, F. Beckert, R. Mülhaupt and C. Janiak, *Nano-Struct. Nano-Objects*, 2015, **2**, 28–34; (*c*) K. P. J. Gustafson, A. Shatskiy, O. Verho, M. D. Kärkäs, B. Schluschass, C.-W. Tai, B. Åkermark, J.-E. Bäckvall and E. V. Johnston, *Catal. Sci. Technol.*, 2017, **7**, 293–299; (*d*) R. Easterday, O. Sanchez-Felix, Y. Losovyj, M. Pink, B. D. Stein, D. G. Morgan, M. Rakitin, V. Y. Doluda, M. G. Sulman, W. E. Mahmoud, A. A. Al-Ghamdi and L. M. Bronstein, *Catal. Sci. Technol.*, 2015, **5**, 1902–1910.
74 A. Bayrami, S. Parvinroo, A. Habibi-Yangjeh and S. Rahim Pouran, *Artif. Cells, Nanomed., Biotechnol.*, 2018, **46**, 730–739.
75 (*a*) D. Gonzalez-Galvez, P. Lara, O. Rivada-Wheelaghan, S. Conejero, B. Chaudret, K. Philippot and P. W. N. M. van Leeuwen, *Catal. Sci. Technol.*, 2013, **3**, 99–105; (*b*) P. Thangavel, B. Viswanath and S. Kim, *Int. J. Nanomed.*, 2017, **12**, 2749–2758.
76 Y.-C. Hsieh, Y. Zhang, D. Su, V. Volkov, R. Si, L. Wu, Y. Zhu, W. An, P. Liu, P. He, S. Ye, R. R. Adzic and J. X. Wang, *Nat. Commun.*, 2013, **4**, 2466.
77 (*a*) P. Kuppusamy, M. M. Yusoff, G. P. Maniam and N. Govindan, *Saudi Pharm. J.*, 2016, **24**, 473–484; (*b*) A. K. Mittal, Y. Chisti and U. C. Banerjee, *Biotechnol. Adv.*, 2013, **31**, 346–356.
78 V. V. Makarov, A. J. Love, O. V. Sinitsyna, S. S. Makarova, I. V. Yaminsky, M. E. Taliansky and N. O. Kalinina, *Acta Naturae*, 2014, **6**, 35–44.
79 A. A. Kajani, A.-K. Bordbar, S. H. Zarkesh Esfahani, A. R. Khosropour and A. Razmjou, *RSC Adv.*, 2014, **4**, 61394–61403.
80 L. Pauksch, S. Hartmann, M. Rohnke, G. Szalay, V. Alt, R. Schnettler and K. S. Lips, *Acta Biomater.*, 2014, **10**, 439–449.
81 A. Jakupec, M. Galanski, V. B. Arion, C. G. Hartinger and B. K. Keppler, *Dalton Trans.*, 2008, 183–194.
82 (*a*) C. S. Joshi, E. S. Priya and C. S. Mathela, *Pharmaceut. Biol.*, 2010, **48**, 206–209; (*b*) K. Loh, *Malays. Fam. Physician*, 2008, **3**, 123; (*c*) M. M. Cohen, *J. Ayurveda Integr. Med.*, 2014, **5**, 251–259; (*d*) D. Rani, P. B. Khare and P. K. Dantu, *Indian J. Pharm. Sci.*, 2010, **72**, 818–822; (*e*) A. Moawad, M. Hetta, J. K. Zjawiony, D. Ferreira and M. Hifnawy, *Nat. Prod. Res.*, 2014, **28**, 41–47; (*f*) C. L. Priya and K. V. Bhaskara Rao, *Pharmacogn. Mag.*, 2016, **12**, S475–S481; (*g*) O. Patel, C. Muller, E. Joubert, J. Louw, B. Rosenkranz and C. Awortwe, *Molecules*, 2016, **21**, 1515.
83 C. P. Kala, P. P. Dhyani and B. S. Sajwan, *J. Ethnobiol. Ethnomed.*, 2006, **2**, 32.
84 (*a*) S. I. Liochev, *Free Radicals Biol. Med.*, 2013, **60**, 1–4; (*b*) P. Davalli, T. Mitic, A. Caporali, A. Lauriola and D. D'Arca, *Oxid. Med. Cell. Longevity*, 2016, **2016**, 3565127; (*c*) C. Giorgi, S. Marchi, I. C. M. Simoes, Z. Ren, G. Morciano, M. Perrone, P. Patalas-Krawczyk, S. Borchard, P. Jędrak, K. Pierzynowska, J. Szymański, D. Q. Wang, P. Portincasa, G. Węgrzyn, H. Zischka, P. Dobrzyn, M. Bonora, J. Duszynski, A. Rimessi, A. Karkucinska-Wieckowska, A. Dobrzyn, G. Szabadkai, B. Zavan, P. J. Oliveira, V. A. Sardao, P. Pinton and M. R. Wieckowski, in *International Review of Cell and Molecular Biology*, ed. C. López-Otín and L. Galluzzi, Academic Press, 2018, vol. 340, pp. 209–344; (*d*) R. M. Palhares, M. Gonçalves Drummond, B. Dos Santos Alves Figueiredo Brasil,

G. Pereira Cosenza, M. das Graças Lins Brandão and G. Oliveira, *PLoS One*, 2015, **10**, e0127866.

85 (*a*) F. Morales, S. Padilla and F. Falconí, *Afr. J. Tradit., Complementary Altern. Med.*, 2016, **14**, 10–15; (*b*) O. Pelkonen, Q. Xu and T.-P. Fan, *Afr. J. Tradit., Complementary Altern. Med.*, 2014, **4**, 1–7; (*c*) N. Jamshidi and M. M. Cohen, *J. Evidence-Based Complementary Altern. Med.*, 2017, **2017**, 13; (*d*) S. M. Mandal, L. Migliolo, S. Das, M. Mandal, O. L. Franco and T. K. Hazra, *J. Cell. Biochem.*, 2012, **113**, 184–193.

86 (*a*) E. Aleebrahim-Dehkordy, H. Nasri, A. Baradaran, P. Nasri, M. R. Tamadon, M. Hedaiaty, S. Beigrezaei and M. Rafieian-Kopaei, *Int. J. Prev. Med.*, 2017, **8**, 96; (*b*) A.-M. Florea and D. Büsselberg, *Cancers*, 2011, **3**, 1351–1371.

87 L. Morris Daniel, *Journal*, 2014, **5**, 397.

88 L. Zeng, P. Gupta, Y. Chen, E. Wang, L. Ji, H. Chao and Z.-S. Chen, *Chem. Soc. Rev.*, 2017, **46**, 5771–5804.

89 C. Irace, G. Misso, A. Capuozzo, M. Piccolo, C. Riccardi, A. Luchini, M. Caraglia, L. Paduano, D. Montesarchio and R. Santamaria, *Sci. Rep.*, 2017, **7**, 45236.

90 U. Jungwirth, C. R. Kowol, B. K. Keppler, C. G. Hartinger, W. Berger and P. Heffeter, *Antioxid. Redox Signaling*, 2011, **15**, 1085–1127.

91 (*a*) J. Creus, J. De Tovar, N. Romero, J. García-Antón, K. Philippot, R. Bofill and X. Sala, *ChemSusChem*, 2019, **12**, 2493–2514; (*b*) Y. Zhao, Y. Luo, X. Yang, Y. Yang and Q. Song, *J. Hazard. Mater.*, 2017, **332**, 124–131; (*c*) X. Zhang and K.-Y. Chan, *Chem. Mater.*, 2003, **15**, 451–459; (*d*) S. P. Somani, P. R. Somani, A. Sato and M. Umeno, *Diamond Relat. Mater.*, 2009, **18**, 497–500; (*e*) J. Sato, N. Saito, Y. Yamada, K. Maeda, T. Takata, J. N. Kondo, M. Hara, H. Kobayashi, K. Domen and Y. Inoue, *J. Am. Chem. Soc.*, 2005, **127**, 4150–4151; (*f*) K. Teramura, K. Maeda, T. Saito, T. Takata, N. Saito, Y. Inoue and K. Domen, *J. Phys. Chem. B*, 2005, **109**, 21915–21921.

92 T. Liu, S. Wang, Q. Zhang, L. Chen, W. Hu and C. M. Li, *Chem. Commun.*, 2018, **54**, 3343–3346.

93 R. B. Nasir Baig and R. S. Varma, *ACS Sustainable Chem. Eng.*, 2013, **1**, 805–809.

94 (*a*) Y. Shvo, I. Goldberg, D. Czerkie, D. Reshef and Z. Stein, *Organometallics*, 1997, **16**, 133–138; (*b*) H. M. Lee, D. C. Smith, Z. He, E. D. Stevens, C. S. Yi and S. P. Nolan, *Organometallics*, 2001, **20**, 794–797.

95 J. P. Boitiaux, J. Cosyns and E. Robert, *Appl. Catal.*, 1987, **32**, 169–183.

96 X. Fang, B. Li, J. Zheng, X. Wang, H. Zhu and Y. Yuan, *Dalton Trans.*, 2019, **48**, 2290–2294.

97 N. Fajrina and M. Tahir, *Int. J. Hydrogen Energy*, 2019, **44**, 540–577.

98 J. Su, J. Zhou, L. Wang, C. Liu and Y. Chen, *Sci. Bull.*, 2017, **62**, 633–644.

99 Y.-T. Kim, P. P. Lopes, S.-A. Park, A. Y. Lee, J. Lim, H. Lee, S. Back, Y. Jung, N. Danilovic, V. Stamenkovic, J. Erlebacher, J. Snyder and N. M. Markovic, *Nat. Commun.*, 2017, **8**, 1449.

100 B. Yao, J. Zhang, X. Fan, J. He and Y. Li, *Small*, 2019, **15**, 1803746.

101 T. Hisatomi and K. Domen, *Nat. Catal.*, 2019, **2**, 387–399.

102 M. Y. Byun, J. S. Kim, J. H. Baek, D.-W. Park and M. S. Lee, *Energies*, 2019, **12**, 284.

103 (*a*) D. K. Mishra, A. A. Dabbawala, J. J. Park, S. H. Jhung and J.-S. Hwang, *Catal. Today*, 2014, **232**, 99–107; (*b*) A. Stolle, T. Gallert, C. Schmöger and B. Ondruschka, *RSC Adv.*, 2013, **3**, 2112–2153; (*c*) D. K. Mishra, A. A. Dabbawala and J.-S. Hwang, *J. Mol. Catal. A: Chem.*, 2013, **376**, 63–70.

104 I. P. Mikheenko, J. Gomez-Bolivar, M. L. Merroun, L. E. Macaskie, S. Sharma, M. Walker, R. A. Hand, B. M. Grail, D. B. Johnson and R. L. Orozco, *Front. Microbiol.*, 2019, **10**, 970.

105 Y. Cheng and S. P. Jiang, *Electrochim. Acta*, 2013, **99**, 124–132.

106 P. T. Anastas and J. C. Warner, *Green Chemistry: Theory and Practice*, Oxford University Press: New York, 1998.